

Interactive comment on “Study of Arabian Red Sea coastal soils as potential mineral dust sources” by P. Jish Prakash et al.

Anonymous Referee #1

Received and published: 25 April 2016

The study presents results from measurements of the mineral composition and other properties of soil, based on 13 samples at four locations in the Saudi Arabian coastal plane adjacent to the Red Sea. The region has been understudied so far, although it is an important source of wind blown dust with at least regional impact on human health, climate, and ecosystems. There is a great need for measurements of this kind, not just in the region studied here, but generally, to better understand the impact of dust aerosols as well as to have more data available, which can be used to evaluate and constrain dust aerosols in modeling studies. Thus, I very welcome this study with the new data. The manuscript is generally well written and well structured. Having said this, I see the potential for some improvement in the manuscript, which can be achieved by doing a minor revision. The study should be published after the recommendations have been taken into account.

The authors apply a variety of measurements techniques for studying the mineral properties of the collected soil samples. This is a good approach, since it allows to study the dust mineral properties from different viewpoints. It also reveals, though, that results from the different types of measurements can vary, allowing for ambiguity in the interpretation. This is most evident in the current study where the mineral composition is investigated for the same size range, i.e., $< 38\mu\text{m}$ particle diameter. For instance, the results from the X-ray diffraction (XRD) analysis give a quartz fraction between about 20 and 40 % and a fraction of all the phyllosilicates of not more than 10%. In contrast, the single particle analysis, using computer controlled scanning electron microscopy, gives a quartz fraction of only

up to about 10%, whereas the phyllosilicates have the largest fraction compared to the other minerals, partially more than 50 %. Which ones of the results from the two different measurement techniques are more reliable? The authors only report these contradicting results next to each other, but a discussion of the significant differences and how to interpret them is lacking. For instance, the possibility of the presence of phyllosilicates in the form amorphous material with poor crystallization is a known source for bias, when XRD analysis is used (*Leinen et al.*, 1994; *Formenti et al.*, 2008; *Kandler et al.*, 2009). Could using this method have caused an overestimation of the quartz fraction? Knowing the answers to such questions would be necessary for properly using the data to constrain or evaluate simulations with dust models.

I recommend following modifications for improving the manuscript:

1. **Section 3, “Sampling and analysis”**: For each of the described measurement techniques applied in the study add information about known sources of bias.

Authors' Response:

Information about known sources of bias has been added to each of the described measurement techniques applied in the study as shown below.

Page 5, Line 23: Minerals with distinctive optical properties, including refractive indices, birefringence, extinction angles, pleochroism, and optical interference patterns, or those showing twinning, distinctive cleavage, and diagnostic extinction angles, can be readily be identified by optical microscopy (Kerr, 1959). Minerals readily identified in these samples by this method include quartz, various feldspars, amphiboles, pyroxenes, micas and carbonates, However, depending on the mineral type, particles <10 µm in diameter are often difficult to identify by this method, including clay minerals and other layered silicates. The method requires the samples preferably to be mounted in epoxy as a polished thin section. The method is biased towards easily identifiable and coarser minerals, especially those with twinning such as feldspars, and showing color and pleochroism such

as hornblende and biotite. The method, although one of the most practical for qualitative mineral analysis, does require mineralogical expertise.

Page 5, Line 31: Powder XRD is particularly suited for fine-grained crystalline mineral mixtures, <10 µm in diameter. The procedure measures the crystallinity of a sample, i.e. excludes amorphous phases such as clay-like colloids (Formenti et al., 2011;Leinen et al., 1994;Engelbrecht et al., 2016;Kandler et al., 2009), partly crystalline layered silicates such as some clays, and hydroxides. If an amorphous phase is present, it will not be fingerprinted by XRD. The assessment of mineral content of a powder sample by the relative intensity ratio (RIR) method suggested by Chung (1974), and as applied in our measurements, does not account for amorphous content.

Page 6, Line 7: This analytical method disperses soil aggregates which are potential dust particles, so shifting the particle size distribution curves towards the smaller particle sizes. This may introduce a bias into the actual size distribution of wind generated dust particles in the field.

Page 6, Line 17: The elemental composition of dust *per se* does not provide adequate information on its mineral content. However, with *a priori* knowledge of the mineral composition of the samples, from optical and XRD measurements, “normative” mineral compositions can be calculated. This provides a method for inter-comparing chemically analyzed samples with each other.

Page 7, Line 10: Due to the attenuation of the electron beam as it impinges the particle surface and loss of energy, the analysis is physically limited to an electron interaction volume of 2–5 µm below the mineral surface, depending on the primary beam voltage and the mineral density (Goldstein et al., 2003). Most of the investigated mineral dust particles have coatings of clay minerals and oxides, which results in an overestimation of the amounts of these minerals when analyzed by CCSEM (Engelbrecht et al., 2009a;Engelbrecht et al., 2016;Engelbrecht et al., 2009b).

2. **Sections 4.3 – 4.5, Figures 3 – 6:** Explicitly state both in the text and in the figures (at the axes or in the captions) the percentages of what variables are shown. Are these the percentages of mass, volume, or number of particles? I suppose it is the mass fraction in the case of the XRD analysis. It is not clear to me in the cases of the other methods.

Authors' Response:

We agree to explicitly state both in the text and in the figures (in the captions) the percentages of variables in section 4.3-4.5 and Figures 3-6.

Section 4.3, Page 8, Line 9: XRD analysis of the thirteen, $D < 38 \mu\text{m}$ sieved samples from the Red Sea coastal plain (Fig. 3) confirmed variable mass percentages of quartz (19 – 44%) and feldspars (plagioclase, K-feldspar) (31 – 48%), as well as of amphibole (and pyroxene) (4 – 31%), lesser amounts of calcite (0.4 – 6.2%), dolomite (1.9 – 6.6%), clays and chlorite (smectite, illite, palygorskite, kaolinite) (3.3 – 8.3%), with traces of gypsum (0 – 0.6%) and halite (0.2 – 4.8%).

Section 4.4, Page 8, Line 23 : The sedimentary samples all contain major mass percentages of SiO_2 , varying between 63% and 78% in the thirteen samples, mostly as the mineral quartz, and lesser mass percentages of Al_2O_3 (3.7 – 7.3 %) CaO (0.9 – 1.7 %), Na_2O (1.2 – 2.0 %), and K_2O (0.9 – 1.6 %), in plagioclase and potassium feldspars. SiO_2 together with Al_2O_3 , Fe_2O_3 (6.5 – 11 %), TiO_2 (1.2 – 2.5 %), MnO (0.1– 0.2 %) MgO (2.3 – 3.1 %), and some K_2O (0.9 – 1.6 %) is also contained in the previously identified amphiboles, clays and micas. Small amounts of CaO (0.9 – 1.7%) are contained in gypsum and calcite, and together with MgO (2.3 – 3.1%), in dolomite.

Section 4.5, Page 9, Line 13: For the total data set, the samples in the 0.5 – 38 μm size range contain by mass about 0.1 – 10.2% quartz, 5 – 54% feldspar, 45 – 72% clay minerals, as major components with lesser amounts of calcite (0.9 – 7.4 %), dolomite (0 – 0.8 %),

gypsum (0 –1.5 %), and iron oxides (0.2 –12.4 %).

Figure 3: Normalized mineral compositions by percentage of mass [quartz (19 – 44%), feldspars (plagioclase, K-feldspar) (31 – 48%), amphibole and pyroxene (4 – 31%), calcite (0.4 – 6.2%), dolomite (1.9 – 6.6%), clays and chlorite (smectite, illite, palygorskite, kaolinite) (3.3 – 8.3%), gypsum (0 – 0.6%) and halite (0.2 – 4.8%)] of thirteen $D < 38\mu\text{m}$ sieved soil samples collected at four localities along the Red Sea coastal area, as measured by X-ray diffraction (XRD).

Figure 4: Compositional plot showing major oxides percentages by mass [SiO_2 (63 – 78%), TiO_2 (1.2 – 2.5 %), Al_2O_3 (3.7 – 7.3 %), Fe_2O_3 (6.5 – 11 %), MgO (2.3 – 3.1 %), CaO (0.9 – 1.7 %), Na_2O (1.2 – 2.0 %), K_2O (0.9 – 1.6 %)] from ICP-OES analysis of $< 38\mu\text{m}$ sieved soils.

Figure 5: CCSEM based individual particle analysis for 0.5 – 38 μm chemical set, with the chemical bins labeled as minerals by mass percentage [Si-rich, Quartz (0.1 – 10.2 %), K Feldspar (2.7 – 15.6 %), Ca Feldspar (1.1 – 25 %); Na Feldspar (1.5 – 13.4 %); Si-Al, Clays (44.7 – 72.1 %); Si-Mg (0 – 3.7 %); Ca-Mg, Dolomite (0 – 0.8 %); Ca-Si (0.6 – 6.4 %); Ca-S, Gypsum (0 – 1.5 %); Ca-rich, Calcite (0.9 – 7.4 %); Fe-rich, Hematite (0.2 – 12.4 %); Salts (0 – 2.2 %); C-rich (0 – 5.5 %) and Misc. (0 – 5.9 %)]

Figure 6: CCSEM based individual particle analysis for 0.5 – 2.5 μm (fine) subset, with the chemical bins labeled as minerals by mass percentage [Si-rich, Quartz (2.1 – 4.9 %), K Feldspar (3.8 – 9.0 %), Na Feldspar (3.8 – 12.9 %); Ca Feldspar (1.4 – 7.7 %); Si-Al, Clays (39.2 – 70.7 %); Si-Mg (0.2 – 1.7 %); Ca-Mg, Dolomite (0 – 0.7 %); Ca-Si (0.3 – 1.5 %); Ca-S, Gypsum (0.1 – 1.7 %); Ca-rich, Calcite (0.6 – 4.1 %); Fe-rich, Hematite (3.2 – 24.1 %); Salts (0.1 – 1.6 %); C-rich (0.4 – 10.5 %) and Miscellaneous. (1.2 – 10.1 %)]

3. Section 5, “Discussion and Conclusions”: Add a discussion of differences in the results

from the different measurement techniques and how these differences should be interpreted. How should the data be used, when they are applied in modeling studies?

Authors' Response:

Discussion of differences in the results from the different measurement techniques has been added and interpreted as follows.

Page 9, line 32: The application of a range of techniques for the analysis of properties of soil samples allows for a better understanding of mineral dust. However, the different analytical methods often provide different results, as seen by comparing the XRD, electron microscopy and chemistry of the soils. In this study, the results from the XRD analysis gives a quartz percentage of between about 19 and 44 % and sheet silicates (clays, micas) of between 3 and about 8%. In contrast, the single particle analysis by CCSEM gives a quartz fraction of only up to about 10%, whereas the sheet silicates always have the largest mineral percentage, of up to about 72%. This can lead to ambiguity in the interpretation of the mineralogical composition of the samples. This is evident even where the mineral composition is investigated for the same size range, i.e. $< 38\mu\text{m}$ particle diameter. Biases in XRD results can be related to the presence of partly amorphous sheet silicates with poor crystallization (Leinen et al., 1994; Formenti et al., 2008; Kandler et al., 2009) and a subsequent overestimation of the quartz fractions. Knowing the answers to such questions would be necessary for properly using the data to constrain or evaluate simulations with dust models. Similarly, the individual particle analysis by CCSEM provides an overestimation of the clay fraction which can be attributed to surface coatings on the quartz and its underestimation (Engelbrecht et al., 2009a, b; Engelbrecht et al., 2016). What is of importance when considering the application of these results in models, health studies, and remote sensing, is not only the mineralogical composition of the dust, but also their mineralogical interrelationships such as mineral clusters, mineral coatings, and intergrowths.

4. **Section 4.1, Page 7, line 32:** Regarding the statement about the satellite images, I suppose this refers to the two references (Jiang et al. and Kalenderski et al.) that are mentioned elsewhere in the manuscript. Please explicitly reference the two papers once more at the end of the sentence.

Authors' Response:

Two references (Jiang et al., 2009 and Kalenderski et al., 2013) have been added in the text as shown below:

Page 7, Line 32, Section 4.1: However, the satellite images (Jiang et al., 2009 and Kalenderski et al., 2013) show that these coastal dust sources are activated quite frequently.

References:

Chung, F. H.: Quantitative interpretation of X-ray diffraction patterns of mixtures. I. Matrix-flushing method for quantitative multicomponent analysis, *Journal of Applied Crystallography*, 7, 519-525, doi:10.1107/S0021889874010375, 1974.

Engelbrecht, J. P., McDonald, E. V., Gillies, J. A., Jayanty, R. K. M., Casuccio, G., and Gertler, A. W.: Characterizing mineral dusts and other aerosols from the Middle East – Part 1: Ambient sampling, *Inhalation Toxicology*, 21, 297-326, 2009a.

Engelbrecht, J. P., McDonald, E. V., Gillies, J. A., Jayanty, R. K. M., Casuccio, G., and Gertler, A. W.: Characterizing mineral dusts and other aerosols from the Middle East – Part 2: Grab samples and re-suspensions, *Inhalation Toxicology*, 21, 327-336, 2009b.

Engelbrecht, J. P., Moosmüller, H., Pincock, S., Jayanty, R. M., Lersch, T., and Casuccio, G.: Technical Note: Mineralogical, chemical, morphological, and optical interrelationships of mineral dust re-suspensions, *Atmospheric Chemistry and Physics, Discussion*, 10.5194/acp-2016-286, 2016.

Formenti, P., J. L. Rajot, K. Desboeufs, S. Caquineau, S. Chevaillier, S. Nava, A. Gaudichet, E. Journet, S. Triquet, S. Alfaro, M. Chiari, J. Haywood, H. Coe, and E. Highwood: Regional variability of the composition of mineral dust from western Africa: Results from the AMMA SOP0/DABEX and DODO field campaigns, *J. Geophys. Res.*, 113, D00C13, doi: 10.1029/2008JD009903, 2008.

Goldstein, J., Newbury, D., Joy, D., Lyman, C., Echlin, P., Lifshin, E., Sawyer, L., and Michael, J.: *Scanning Electron Microscopy and X-Ray Microanalysis: 3rd Edition*, Springer, 689 pp., 2003.

Jiang, H., Farrar, J. T., Beardsley, R. C., Chen, R., and Chen, C.: Zonal surface wind jets across the Red Sea due to mountain gap forcing along both sides of the Red Sea, *Geophys. Res. Lett.*, 36, L19605, 10.1029/2009GL040008, 2009.

Kalenderski, S., Stenchikov, G., and Zhao, C.: Modeling a typical winter-time dust event over the Arabian Peninsula and the Red Sea, *Atmos. Chem. Phys.*, 13, 1999-2014, 10.5194/acp-13-1999-2013, 2013.

Kandler, K., L. Schütz, C. Deutscher, M. Ebert, H. Hofmann, S. Jäckel, R. Jaenicke, P. Knipertz, K. Lieke, A. Massling, A. Petzold, A. Schladitz, B. Weinzierl, A. Wiedensohler, S. Zorn, and S. Weinbruch: Size distribution, mass concentration, chemical and mineralogical composition and derived optical parameters of the boundary layer aerosol at Tinfou, Morocco, during SAMUM 2006, *Tellus B*, 61(1), 32–50, doi:10.1111/j.1600-0889.2008.00385.x., 2009.

, !!! INVALID CITATION !!! (Formenti et al., 2011;Leinen et al., 1994;Engelbrecht et al., 2016;Kandler et al., 2009).

Aba-Husayn, M. M., Dixon, J. B., and Lee, S. Y.: Mineralogy of Saudi Arabian Soils: Southwestern Region, *Soil Science Society of America Journal*, 44, 643-649, 10.2136/sssaj1980.03615995004400030043x, 1980.

Acosta, F., Ngugi, D. K., and Stingl, U.: Diversity of picoeukaryotes at an oligotrophic site off the Northeastern Red Sea Coast, *Aquatic Biosystems*, 9, 10.1186/2046-9063-9-16, 2013.

Al-Dabbas, M. A., Ayad Abbas, M., and Al-Khafaji, R. M.: Dust storms loads analyses-Iraq, *Arabian Journal of Geosciences*, 5, 121-131, 10.1007/s12517-010-0181-7, 2012.

Al-Dousari, A., and Al-Awadhi, J.: Dust fallout in northern Kuwait, major sources and characteristics, *Kuwait Journal of Science & Engineering*, 39(2A), 171-187, 2012.

Al-Farraj, A. S.: The mineralogy of clay fractions in the soils of the southern region of Jazan, Saudi Arabia, *Journal of Agronomy*, 7, 115-126, 2008.

Bennett, C. M., McKendry, I. G., Kelly, S., Denike, K., and Koch, T.: Impact of the 1998 Gobi dust event on hospital admissions in the Lower Fraser Valley, British Columbia, *Sci. Total Environ.*, 366, 918-925, 10.1016/j.scitotenv.2005.12.025, 2006.

Bennion, P., Hubbard, R., O'Hara, S., Wiggs, G., Wegerdt, J., Lewis, S., Small, I., van der Meer, J., and Upshur, R.: The impact of airborne dust on respiratory health in children living in the Aral Sea region, *Int. J. Epidemiol.*, 36, 1103-1110, 10.1093/ije/dym195, 2007.

Brindley, H., Osipov, S., Bantges, R., Smirnov, A., Banks, J., Levy, R., Jish Prakash, P., and Stenichkov, G.: An assessment of the quality of aerosol retrievals over the Red Sea and evaluation of the climatological cloud-free dust direct radiative effect in the region, *J. Geophys. Res.: Atmos.*, 120, 2015JD023282, 10.1002/2015JD023282, 2015.

Buseck, P. R., Jacob, D. J., Pósfai, M., Li, J., and Anderson, J. R.: Minerals in the air: An environmental perspective, *International Geology Review, Symposium*, Stanford, California, 1999.

Caquineau, S., Magonthier, M.-C., Gaudichet, A., and Gomes, L.: An improved procedure for the X-ray diffraction analysis of low-mass atmospheric dust samples, *European Journal of Mineralogy*, 9, 157-166, 1997.

Chung, F. H.: Quantitative interpretation of X-ray diffraction patterns of mixtures. I. Matrix-flushing method for quantitative multicomponent analysis, *Journal of Applied Crystallography*, 7, 519-525, doi:10.1107/S0021889874010375 1974.

De Longueville, F., Hountondji, Y. C., Henry, S., and Ozer, P.: What do we know about effects of desert dust on air quality and human health in West Africa compared to other regions?, *Science of the Total Environment*, 409, 1-8, 2010.

Edgell, H. S.: *Arabian Deserts. Nature, Origin and Evolution*, Springer, Dordrecht, Netherlands, 592 pp., 2006.

Engelbrecht, J. P., McDonald, E. V., Gillies, J. A., Jayanty, R. K. M., Casuccio, G., and Gertler, A. W.: Characterizing mineral dusts and other aerosols from the Middle East – Part 1: Ambient sampling, *Inhalation Toxicology*, 21, 297-326, 2009a.

Engelbrecht, J. P., McDonald, E. V., Gillies, J. A., Jayanty, R. K. M., Casuccio, G., and Gertler, A. W.: Characterizing mineral dusts and other aerosols from the Middle East – Part 2: Grab samples and re-suspensions, *Inhalation Toxicology*, 21, 327-336, 2009b.

Engelbrecht, J. P., Gillies, J. A., Etyemezian, V., Kuhns, H., Baker, S. E., Zhu, D., Nikolich, G., and Kohl, S. D.: Controls on mineral dust emissions at four arid locations in the western USA, *Aeolian Research*, 6, 41-54, 2012.

Engelbrecht, J. P., and Moosmüller, H.: *Mobile Aerosol Monitoring System for Department of Defense - Continuous Aerosol and Aerosol Optics Measurement in Theater*, U.S. Army Medical Research and Materiel Command, Fort Detrick, Maryland Report W81XWH-11-2-0220, 1-229, 2014.

Engelbrecht, J. P., Moosmüller, H., Pincock, S., Jayanty, R. M., Lersch, T., and Casuccio, G.: Technical Note: Mineralogical, chemical, morphological, and optical interrelationships of mineral dust re-suspensions, *Atmospheric Chemistry and Physics, Discussion*, 10.5194/acp-2016-286, 2016.

Esteve, V., Rius, J., Ochando, L. E., and Amigó, J. M.: Quantitative x-ray diffraction phase analysis of coarse airborne particulate collected by cascade impactor sampling, *Atmospheric Environment* 31, 3963-3967, doi:10.1016/S1352-2310(97)00257-4 1997.

Formenti, P., Schütz, L., Balkanski, Y., Desboeufs, K., Ebert, M., Kandler, K., Petzold, A., Scheuvens, D., Weinbruch, S., and Zhang, D.: Recent progress in understanding physical and

chemical properties of African and Asian mineral dust, *Atmospheric Chemistry and Physics*, 11, 8231-8256, 10.5194/acp-11-8231-2011, 2011.

Fryrear, D. W.: Long-term effect of erosion and cropping on soil productivity, *Spec. Pap. - Geol. Soc. Am.*, 186, 253-260, 10.1130/SPE186-p253, 1981.

Gee, G. W., and Or, D.: Particle-size analysis, in: *Methods of Soil Analysis: Part 4—Physical Methods*, No. 5, edited by: Dane, J. H., and Topp, G. C., Soil Science Society of America, Madison, WI., 255-293, 2002.

Gillette, D. A., and Walker, T. R.: Characteristics of airborne particles produced by wind erosion of sandy soil, *High Plains of West Texas*, *Soil Science*, 123, 97-110, 1977.

Goldstein, J., Newbury, D., Joy, D., Lyman, C., Echlin, P., Lifshin, E., Sawyer, L., and Michael, J.: *Scanning Electron Microscopy and X-Ray Microanalysis: 3rd Edition*, Springer, 689 pp., 2003.

Goudie, A. S., and Middleton, N.J.: *Desert Dust in the Global System*, Springer, 287 pp., 2006.

Grainger, D.: *The Geological Evolution of Saudi Arabia, a Voyage through Space and Time* Saudi Geological Survey, 2007.

Greely, R., and Iversen, J. D.: *Wind as a geological process on Earth, Mars, and Venus*, Cambridge University Press, Cambridge, 333 pp., 1985.

Grell, G., Peckham, S. E., Schmitz, R. A., M. S., Frost, G., Skamarock, W. C., and Eder, B.: Fully coupled "online" chemistry within the WRF Model, *Atmos. Env.*, 39, 6957-6975, 2005.

Guerzoni, S., Molinaroli, E., and Chester, R.: Saharan dust inputs to the western Mediterranean Sea: depositional patterns, geochemistry and sedimentological implications, *Deep Sea Res., Part II*, 44, 631-654, 1997.

Hagen, L. J., and Woodruff, N. P.: Air pollution from dust storms in the Great Plains, *Atmos. Env.*, 7, 323-332, 1973.

Haywood, J., and Boucher, O.: Estimates of the direct and indirect radiative forcing due to tropospheric aerosols: A review, *Rev. Geophys.*, 38, 513-543, 10.1029/1999RG000078, 2000.

Hsu, N. C., Tsay, S. C., King, M. D., and Herman, J. R.: Aerosol properties over bright-reflecting source regions, *IEEE Trans. Geosci.*, 42, 557-569, 2004.

Huang, J., Minnis, P., Lin, B., Wang, T., Yi, Y., Hu, Y., Sun-Mack, S., and Ayers, K.: Possible influences of Asian dust aerosols on cloud properties and radiative forcing observed from MODIS and CERES, *Geophys. Res. Lett.*, 33, L06824, 10.1029/2005GL024724, 2006.

Huang, J., Wang, T., Wang, W., Li, Z., and Yan, H.: Climate effects of dust aerosols over East Asian arid and semiarid regions, *J. Geophys. Res.: Atmos.*, 119, 2014JD021796, 10.1002/2014JD021796, 2014.

Jiang, H., Farrar, J. T., Beardsley, R. C., Chen, R., and Chen, C.: Zonal surface wind jets across the Red Sea due to mountain gap forcing along both sides of the Red Sea, *Geophys. Res. Lett.*, 36, L19605, 10.1029/2009GL040008, 2009.

Jickells, T. D., An, Z. S., Andersen, K. K., Baker, A. R., Bergametti, G., Brooks, N., Cao, J. J., Boyd, P. W., Duce, R. A., Hunter, K. A., Kawahata, H., Kubilay, N., laRoche, J., Liss, P. S., Mahowald, N., Prospero, J. M., Ridgwell, A. J., Tegen, I., and Torres, R.: Global iron connections between desert dust, ocean biogeochemistry, and climate, *Science*, 308, 67-71, 2005.

Kalenderski, S., Stenchikov, G., and Zhao, C.: Modeling a typical winter-time dust event over the Arabian Peninsula and the Red Sea, *Atmos. Chem. Phys.*, 13, 1999-2014, 10.5194/acp-13-1999-2013, 2013.

Kandler, K., Schütz, L., Deutscher, C., Ebert, M., Hofmann, H., Jäckel, S., Jaenicke, R., Knippertz, P., Lieke, K., Massling, A., Petzold, A., Schladitz, A., Weinzierl, B., Wiedensohler, A., Zorn, S., and Weinbruch, S.: Size distribution, mass concentration, chemical and mineralogical composition

and derived optical parameters of the boundary layer aerosol at Tinfou, Morocco, during SAMUM 2006, *Tellus*, 61B, 32-50, 2009.

Kerr, P. F.: *Optical Mineralogy*, 3rd ed., McGraw-Hill Book Company, Inc., 442 pp., 1959.

Kok, J. F.: Does the size distribution of mineral dust aerosols depend on the wind speed at emission?, *Atmos. Chem. Phys.*, 11, 10149–10156, 2011a.

Kok, J. F.: A scaling theory for the size distribution of emitted dust aerosols suggests climate models underestimate the size of the global dust cycle, *Proc. Natl. Acad. Sci.*, 108, 1016–1021, 2011b.

Kumar, R., Barth, M. C., Pfister, G. G., Naja, M., and Brasseur, G. P.: WRF-Chem simulations of a typical pre-monsoon dust storm in northern India: influences on aerosol optical properties and radiation budget, *Atmos. Chem. Phys.*, 14, 2431-2446, 10.5194/acp-14-2431-2014, 2014.

Lee, S. Y., Dixon, J. B., and Aba-Husayn, M. M.: Mineralogy of Saudi Arabian Soils: Eastern Region, *Soil Science Society of America Journal*, 47, 321-326, 10.2136/sssaj1983.03615995004700020030x, 1983.

Leinen, M., Prospero, J. M., Arnold, E., and Blank, M.: Mineralogy of aeolian dust reaching the North Pacific Ocean 1. Sampling and analysis, *Journal of Geophysical Research*, 99, 21,017-021,023, 1994.

Mahowald, N., S. Engelstaedter, C. Luo, A. Sealy, P. Artaxo, C. Benitez-Nelson, S. Bonnet, Y. Chen, P.Y. Chuang, D.D. Cohen, F. Dulac, B. Herut, A.M. Johansen, N. Kubilay, R. Losno, W. Maenhaut, A. Paytan, J.M. Prospero, L.M. Shank, and R.L. Siefert: Atmospheric iron deposition: Global distribution, variability and human perturbations, *Annual Reviews of Marine Sciences*, 1, 245-278, 2009.

Marticorena, B., and Bergametti, G.: Modeling the atmospheric dust cycle: 1. Design of a soil-derived dust emission scheme, *J. Geophys. Res.: Atmos.*, 100, 16415-16430, 10.1029/95JD00690, 1995.

Marticorena, B.: Dust production mechanisms, in: *Mineral Dust: A Key Player in the Earth System*, edited by: Knippertz, P., and Stuut, J.-B. W., Springer Science+Business Media Dordrecht, 93-120, 2014.

Menéndez, I., Pérez-Chacón, E., Mangas, J., Tauler, E., Engelbrecht, J. P., Derbyshire, E., Cana, L., and Alonso, I.: Dust deposits on La Graciosa Island (Canary Islands, Spain): Texture, mineralogy and a case study of recent dust plume transport, *Catena*, 117, 133-144, 2014.

Menut, L., Pérez, C., Haustein, K., Bessagnet, B., Prigent, C., and Alfaro, S.: Impact of surface roughness and soil texture on mineral dust emission fluxes modeling, *J. Geophys. Res.: Atmos.*, 118, 6505-6520, 10.1002/jgrd.50313, 2013.

Migon, C., Sandroni, V., and Béthoux, J. P.: Atmospheric input of anthropogenic phosphorus to the northwest Mediterranean under oligotrophic conditions, *Marine Environmental Research*, 7, 1-14., 2001.

Moosmüller, H., Engelbrecht, J. P., Skiba, M., Frey, G., Chakrabarty, R. K., and Arnott, W. P.: Single scattering albedo of fine mineral dust aerosols controlled by iron concentration, *J. Geophys. Res.*, 117, D11210, doi:10.1029/2011JD016909, 10.1029/2011JD016909, 2012.

Muhs, D. R., Prospero, J. M., Baddock, M. C., and Gill, T. E.: Identifying sources of aeolian mineral dust: Present and past, in: *Mineral Dust, A Key Player in the Earth System*, edited by: Knippertz, P., and Stuut, J.-B. W., Springer Science+Business Media Dordrecht, 51-74, 2014.

Nickovic, S., Vukovic, A., Vujadinovic, M., Djurdjevic, V., and Pejanovic, G.: Technical Note: High-resolution mineralogical database of dust-productive soils for atmospheric dust modeling, *Atmospheric Chemistry and Physics*, 12, 845–855, 2012.

Nihlen, T., and Lund, S. O.: Influence of Aeolian Dust on Soil Formation in the Aegean Area, *Z. Geomorphol.*, 393, 341-361, 1995.

Oleson, K. W., Lawrence, D. M., Bonan, G. B., Flanner, M. G., Kluzek, E., Lawrence, P. J., Levis, S., Swenson, S. C., Thornton, P. E., Dai, A., Decker, M., Dickinson, R., Feddema, J., Heald, C. L., Hoffman, F., Lamarque, J., Mahowald, N., Niu, G., Qian, T., Randerson, J., Running, S., Sakaguchi, K., Slater, A., Stockli, R., Wang, A., Yang, Z., Zeng, X., and Zeng, X.: Technical Description of version 4.0 of the Community Land Model (CLM). , NCAR Technical Note NCAR/TN-478+STR, 2010.

Osipov, S., Stenchikov, G., Brindley, H., and Banks, J.: Diurnal cycle of the dust instantaneous direct radiative forcing over the Arabian Peninsula, *Atmos. Chem. Phys.*, 15, 9537-9553, 10.5194/acp-15-9537-2015, 2015.

Perlwitz, J. P., Pérez García-Pando, C., and Miller, R. L.: Predicting the mineral composition of dust aerosols – Part 1: Representing key processes, *Atmos. Chem. Phys.*, 15, 11593-11627, 10.5194/acp-15-11593-2015, 2015a.

Perlwitz, J. P., Pérez García-Pando, C., and Miller, R. L.: Predicting the mineral composition of dust aerosols – Part 2: Model evaluation and identification of key processes with observations, *Atmos. Chem. Phys.*, 15, 11629-11652, 10.5194/acp-15-11629-2015, 2015b.

Prakash, J. P., Stenchikov, G., Kalenderski, S., Osipov, S., and Bangalath, H.: The impact of dust storms on the Arabian Peninsula and the Red Sea, *Atmos. Chem. Phys.*, 15, 199-222, 10.5194/acp-15-199-2015, 2015.

Prospero, J. M., Ginoux, P., Torres, O., Nicholson, S. E., and Gill, T. E.: Environmental characterization of global sources of atmospheric soil dust identified with the NIMBUS 7 total ozone mapping spectrometer (TOMS) absorbing aerosol product, *Rev. Geophys.*, 40, 31, 10.1029/2000RG000095, 2002.

Pye, K.: Aeolian dust and dust deposits, Academic Press, London, 1987.

Rietveld, H. M.: A profile refinement method for nuclear and magnetic structures, *Journal of Applied Crystallography*, 2, 65-71, dx.doi.org/10.1107/S0021889869006558, 1969.

Scheuvs, D., and Kandler, K.: On composition, morphology, and size distribution of airborne mineral dust, in: *Mineral Dust, a Key Player in the Earth System*, edited by: Knippertz, P., and Stuut, J.-B. W., Springer Science+Business Media Dordrecht, 15-49, 2014.

Shadfan, H., Mashhady, A., Eter, A., and Hussen, A. A.: Mineral composition of selected soils in Saudi Arabia, *Journal of Plant Nutrition and Soil Science*, 147, 657-668, 10.1002/jpln.19841470603, 1984.

Sokolik, I. N., and Toon, O. B.: Direct radiative forcing by anthropogenic airborne mineral aerosols, *Nature*, 381, 681-683, 1996.

Sokolik, I. N., and Toon, O. B.: Incorporation of mineralogical composition into models of the radiative properties of mineral aerosol from UV to IR wavelengths, *J. Geophys. Res.: Atmos.*, 104, 9423-9444, 10.1029/1998JD200048, 1999.

Sturges, W. T., Harrison, R. M., and Barrie, L. A.: Semi-quantitative X-ray diffraction analysis of size fractionated atmospheric particles, *Atmos. Env.*, 23, 1083-1098, 1989.

Tanaka, T. Y., and Chiba, M.: A numerical study of the contributions of dust source regions to the global dust budget, *Global and Planetary Change*, 52, 88-104, 2006.

Tegen, I., and Fung, I.: Contribution to the atmospheric mineral aerosol load from land surface modification, *Journal of Geophysical Research*, 100, 18707-18726, 1995.

Twomey, S. A., Piegras, M., and Wolfe, T. L.: An assessment of the impact of pollution on global cloud albedo, *Tellus B*, 36, 10.3402/tellusb.v36i5.14916, 2011.

UCAR/NCAR: Forecasting Dust Storms, National Center for Atmospheric Research, Boulder, National Center for Atmospheric Research, Boulder, 1-67, 2003.

Viani, B. E., A. S. Al-Mashhady, and Dixon, J. B.: Mineralogy of Saudi Arabian Soils: Central Alluvial Basins, *Soil Science Society of America Journal*, 47, 149-157, 10.2136/sssaj1983.03615995004700010030x, 1983.

Wang, W., Huang, J., Minnis, P., Hu, Y., Li, J., Huang, Z., Ayers, J. K., and Wang, T.: Dusty cloud properties and radiative forcing over dust source and downwind regions derived from A-Train data during the Pacific Dust Experiment, *J. Geophys. Res.: Atmos.*, 115, D00H35, 10.1029/2010JD014109, 2010.

Wang, Z., Ueda, H., and Huang, M.: A deflation module for use in modeling long-range transport of yellow sand over East Asia, *J. Geophys. Res.: Atmos.*, 105, 26947-26959, 10.1029/2000JD900370, 2000.

Washington, R., Todd, M. C., Middleton, N. J., and Goudie, A. S.: Dust-storm source areas determined by the total ozone monitoring spectrometer and surface observations, *Annals of the Association of American Geographers*, 93, 297-313, 2003.

Washington, R., and Todd, M. C.: Atmospheric controls on mineral dust emission from the Bodélé depression, Chad: The role of the low level jet, *Geophysical Research Letters*, 32, L17701, doi:10.1029/2005GL023597, 2005.

Webb, N. P., and Strong, C. L.: Soil erodibility dynamics and its representation for wind erosion and dust emission models, *Aeolian Res.*, 3, 165-179, 10.1016/j.aeolia.2011.03.002, 2011.

Weese, C. B., and Abraham, J. H.: Potential health implications associated with particulate matter exposure in deployed settings in Southwest Asia, *Inhalation Toxicology*, 21, 291-296, 2009.

Zender, C. S., Huiheng, B., and David, N.: Mineral Dust Entrainment and Deposition (DEAD) model: Description and 1990s dust climatology, *J. Geophys. Res.: Atmos.*, 108, 2003.

Leinen, M., J. M. Prospero, E. Arnold, and M. Blank: Mineralogy of aeolian dust reaching the north Pacific Ocean 1. sampling and analysis, *J. Geophys. Res.*, 99(D10), 21,017–21,023, doi:10.1029/94JD01735, 1994.

Interactive comment on “Study of Arabian Red Sea coastal soils as potential mineral dust sources” by P. Jish Prakash et al.

K. Kandler (Referee)

kzk@gmx.de

Received and published: 28 June 2016

The present publication deals with soils in potential dust sources close to the Arabian Sea, an area, of which only few data exists. Mineralogical and geochemical analyses of the potentially windblown size fraction have been investigated. The paper adds new data interesting for atmospheric research. Similar to the anonymous reviewer, I also would like to see a more critical assessment and comparison of the results from the different techniques. Moreover, a placement of the composition data with regard to other dust source regions would be desirable.

Authors' response:

We added a critical assessment and comparison of the results, as also recommended by Reviewer 1 (see Authors' Response to Reviewer 1). We also added a comparative chemical results from other dust regions

Major remarks

page 4/lines 10-27: The “objectives” chapter apart from first and last sentence, doesn't really contain any clear objectives, but a mixture of introduction and general information. I suggest rewriting it and clearly stating the goals of the present study. Any introductory information and motivation should go to chapter 1.

Authors' response:

The introductory information was moved from the objectives to the introductory section. Parts of the objectives section were re-compiled to better describe our objectives

9/31: As of now, I suggest terming it rather “Summary and conclusions”, as there is not much discussion here.

Authors' response:

The heading was change to “Summary and conclusions” as suggested.

9/32-10/13: This information belongs rather in introduction. Please merge. In chapter 4 there is some detailed information of the separate samples, and some intercomparison of the samples. However, I'm somewhat missing a comparison with previous measurements from other regions. Are these sources different to Eastern and Western African, Sahelian, or even Chinese sources? There's for example the reviews of Formenti et al. (2011) and Scheuven et al. (2013), where data for comparison is readily available, e.g. in terms of mineral and elemental ratios. Or maybe the authors can provide more information on other sources by themselves or use the mentioned databases?

Authors' response:

The mentioned text was moved to and re-compiled in the introduction. Comparative chemical results from adjacent regions, together with references were included in section 4.4 as suggested, specifically the Fe/Al ratios. Si/Al, Ca/Al, and Fe/Al ratios are included in the two tables in Appendix A.

Fig. 3 and 5: Data from SEM and XRD are apparently different, when displayed this way. If SEM data shows particle number percent, I would highly suggest calculating mass percentages from them (by assuming spherical or ellipsoidal particles and assigning an according bulk density) and compare again with XRD data. Differences should be discussed. Is there any chemical fingerprint that can be used to detect amphibole in SEM data?

Authors' response:

The SEM results are in mass percentages. The headings of Figures 5 and 6 have been corrected to reflect this correction. We have added a discussion on the differences between the results generated by the different techniques. No chemical fingerprint for amphibole had been identified from our analyses.

Minor / corrections

page 2/line 13: It's not just the resolution of the databases limiting statements, but also the general lack of soil data.

Authors' response:

The sentence was rephrased to include the general lack of soil data

2/14-34: The explanation of a source function doesn't seem to contribute to the rest of the manuscript, except for explaining the particle size range of interest. As the latter can be done with a single reference, I suggest removing it.

Authors' response:

We prefer to retain the source function, since it mentions parameters such as particle size distribution which we analyzed and consider to be important

2/19-29: Please discuss the parameters in order of appearance, and do not jump from one to the other and back.

Authors' response:

We changed the order in which the parameters are discussed so as to be in the order that they appear in the equation

2/33-34: It seems to me that this motivation sentence should rather be at the beginning of the section.

Authors' response:

We moved this to the beginning of the section, as suggested

3/4-26: This is a lot of information, which is difficult to assess for the reader. If you think it is necessary for the present manuscript, I would suggest trying a graphical representation. Otherwise, I suggest restricting it to the information relevant for the current sampling area.

Authors' response:

We deleted the information not specifically close to the sampling region, retaining those on the southwestern part of the Arabian Peninsula.

3/27-4/9: I assume this information is from literature. Please add reference(s).

Authors' response:

We believe the information presented in this part of the paper is sufficiently supported by the existing references

4/16-18: Which observation? Please be more specific and include references, if appropriate.

Authors' response:

This section was moved to the introduction and references added "MODIS and SEVIRI satellite observations"

4-29-5/4: I would assume that precise geographical coordinates would be available for all sampling locations. Please add them, at least to a supplement. That could be done as a table.

Authors' response:

These are listed in Table 1

5/5-9: This information should be location in the introduction, as it has nothing to do with sampling and analysis.

Authors' response:
Moved text to introduction

5/11: Which unwanted artifacts?

Authors' response:
Replaced the word with "detritus"

5/21-23: General information, omit or place in introduction.

Authors' response:
Moved to introduction

5/25-27: General information, omit or place in introduction.

Authors' response:
Moved to introduction

5/34-6/2: General information, omit or place in introduction.

Authors' response:
Moved to introduction

6/13-15 and 6/19-21: The chemical symbols are sufficient, there is no concern of ambiguity.

Authors' response:
For the benefit of non-chemists we prefer to retain the chemical names and symbols, e.g. iron (Fe)

6/24-25: General information, omit or place in introduction.

Authors' response:
Moved to introduction

6/33: rastering -> scanning?

Authors' response:
We retained the word "rastering" as it is used as such in electron microscopy, meaning scanning along a two dimensional grid

7/1: $0.5 \mu\text{m} < D < 38 \mu\text{m}$

Authors' response:
Corrected

7/29: disaggregation?

Authors' response:
Corrected to read "disaggregation"

8/3: eroded?

Authors' response:
The spelling was corrected

9/6: Is it 2000 particles per sample?

Authors' response:
We corrected this to read 2000 particles per sample

9/6-12: On which substrate this analysis was performed, and how were the C-rich identified, if on carbonaceous material?

Authors' response:
Polycarbonate substrate was used for the CCSEM analysis. The C rich particles often contain minor amounts of other elements such as sulfur and metals, allowing them to be identified by their backscattered electron image. However, we admit this can be a real challenge and of course impossible to identify if they contain only C.

Fig. B1 and B2: please combine them into a single (or two) color figure(s), as without any grid the small differences are hard to spot. I suggest giving the size and shape statistics as separate table.

Authors' response:
Figure 7 provides an average size distribution and summary statistics. The statistics for individual samples are given in the two tables of Appendix A. Individual sample particle size distribution plots are moved out of the manuscript *per se*, into Supplementary Information section.

Fig. B3: I suggest either removing, as 4 images do not really represent variation in composition and morphology, or making better use of, e.g. by discussion specific details and characteristics of the particles.

Authors' response:
The 4 SEM images are moved out of the manuscript into Supplementary Information section

Formenti, P., L. Schütz, Y. Balkanski, K. Desboeufs, M. Ebert, K. Kandler, A. Petzold, D. Scheuven, S. Weinbruch, D. Zhang (2011): Recent progress in understanding physical and chemical properties of mineral dust. *Atmos. Chem. Phys.* 11, 8231-8256. doi: 10.5194/acp-11-8231-2011

Scheuven, D., L. Schütz, K. Kandler, M. Ebert, S. Weinbruch (2013): Bulk composition of northern African dust and its source sediments - a compilation. *Earth-Sci. Rev.* 116, 170-194. doi: 10.1016/j.earscirev.2012.08.005

Interactive comment on *Atmos. Chem. Phys. Discuss.*, doi:10.5194/acp-2016-113, 2016.

1 **Arabian Red Sea coastal soils as potential mineral dust sources**
2 **P. Jish Prakash¹, Georgiy Stenchikov¹, Weichun Tao¹, Tahir Yapici¹, Bashir Warsama¹,**
3 **and Johann Engelbrecht^{2,1}**

4 [1] King Abdullah University of Science and Technology (KAUST), Physical Science and
5 Engineering Division (PSE), Thuwal, 23955-6900, Saudi Arabia.

6 [2] Desert Research Institute (DRI), Reno, Nevada 89512-1095, U.S.A.

7 Correspondence to P. Jish Prakash (jishprakash@gmail.com)

8

1 Abstract

2 Both Moderate Resolution Imaging Spectroradiometer (MODIS) and Spinning Enhanced Visible
3 and InfraRed Imager (SEVIRI) satellite observations suggest that the narrow heterogeneous Red
4 Sea coastal region is a frequent source of airborne dust that, because of its proximity, directly
5 affects the Red Sea and coastal urban centers. The potential of soils to be suspended as airborne
6 mineral dust depends largely on soil texture, moisture content, and particle size distributions.
7 Airborne dust inevitably carries the mineralogical and chemical signature of a parent soil. The
8 existing soil databases are too coarse to resolve the small but important coastal region. The
9 purpose of this study is to better characterize the mineralogical, chemical and physical properties
10 of soils from the Red Sea Arabian coastal plane, which in turn will help to improve assessment
11 of dust effect on the Red Sea and land environmental systems and urban centers. Thirteen surface
12 soils from the hot-spot areas of wind-blown mineral dust along the Red Sea coastal plain were
13 sampled for analysis. Analytical methods included Optical Microscopy, X-ray diffraction
14 (XRD), Inductively Coupled Plasma Optical Emission Spectrometry (ICP-OES), Ion
15 Chromatography (IC), Scanning Electron Microscopy (SEM), and Laser Particle Size Analysis
16 (LPSA). We found that the Red Sea coastal soils contain major components of quartz and
17 feldspar, as well as lesser but variable amounts of amphibole, pyroxene, carbonate, clays, and
18 micas, with traces of gypsum, halite, chlorite, epidote and oxides. The ~~wide~~ range of minerals in
19 the soil samples was ascribed to the variety of igneous and metamorphic provenance rocks of the
20 Arabian Shield forming the escarpment to the east of the Red Sea coastal plain. The analysis
21 revealed that the samples contain compounds of nitrogen, phosphorus and iron that are essential
22 nutrients to marine life. The analytical results from this study will provide a valuable input into
23 dust emission models used in climate, marine ecology, and air-quality studies.

24 **Key words:** Dust mineralogy; ~~Dust chemistry~~Chemical composition; Soil grab samples; Saudi
25 Arabian dust

26 1. Introduction

27 Mineral dust is the most abundant atmospheric aerosol, primarily suspended from ground in arid
28 and semi-arid regions of the globe (Buseck et al., 1999; Washington and Todd, 2005; Goudie,
29 2006; Muhs et al., 2014), including deserts of the Arabian Peninsula (Edgell, 2006). Dust aerosols
30 profoundly affect climate, biogeochemical cycles in the ocean and over land, air-quality,
31 atmospheric chemistry, cloud formation, visibility, and human activities (Prospero et al.,
32 2002; Haywood and Boucher, 2000; Hsu et al., 2004; Sokolik and Toon, 1999; Kumar et al.,
33 2014; De Longueville et al., 2010; Jickells et al., 2005; Mahowald, 2009; Huang et al., 2006; Huang
34 et al., 2014; Fryrear, 1981; Nihlen and Lund, 1995; Hagen and Woodruff, 1973; Bennett et al.,
35 2006; Bennion et al., 2007; Twomey et al., 2011; Wang et al., 2010). The Arabian Peninsula is one
36 of Earth's major sources of atmospheric dust, which contributes as much as 11.8% (22 – 500
37 Mt/a) of the total (1,877 – 4000 Mt/a) global dust emissions (Tanaka and Chiba, 2006). The Red
38 Sea surrounded by African and Arabian deserts is strongly affected by dust. Along with profound
39 impact on the surface energy budget over land and ~~over~~ the sSea (Brindley et al.,
40 2015; Kalenderski et al., 2013; Osipov et al., 2015), dust is an important source of nutrients
41 especially for the oligotrophic northern Red Sea region (Acosta et al., 2013). Dust affects marine
42 life, also controlling incoming solar and terrestrial radiation. The coastal plains of the Arabian
43 Peninsula along the Red Sea and Persian Gulf are among the most populated areas in this region
44 hosting the major industrial and urban centers.

1 Both Moderate Resolution Imaging Spectroradiometer (MODIS) and Spinning Enhanced Visible
2 and InfraRed Imager (SEVIRI) satellite observations suggest that the narrow Red Sea coastal
3 belt is an important dust source region, augmented by the fine-scale sediment accumulations,
4 scattered vegetation, and varying terrain. D~~The dust hot spots are located within the narrow~~
5 coastal region, and because of their proximity to the Red Sea, contribute to the dust/nutrient
6 balance of the s~~Sea, during both dusty and fair weather conditions. The coastal plains of the~~
7 Arabian Peninsula along the Red Sea and Persian Gulf are among the most populated areas in
8 this region hosting the major industrial and urban centers.
9 Airborne dust profoundly affects human activities, marine and land ecosystems, climate, air-
10 quality, and human health. The observations suggest that the narrow Red Sea coastal belt is an
11 important dust source region, augmented by the fine scale sediment accumulations, scattered
12 vegetation, and varying terrain.
13 Dust emission rates from soils and sites of airborne particles strongly depend on the soil particle
14 size distributions. Optical properties such as scattering, absorption and refractive indices vary by
15 mineralogical content and particle size of the dust in the atmosphere. Dust reactivity in the
16 seawater also depends on their mineralogy, e.g. carbonates (calcite, dolomite), evaporites
17 (gypsum) and some oxides (hematite, goethite) are generally more soluble in water than for
18 example most silicates (quartz, feldspars, micas, clays, amphiboles, or pyroxenes). Soils in arid
19 regions are most susceptible to wind erosion, where particles are only loosely bound to the
20 surface by the low soil moisture or being physically disturbed by agriculture or traffic. Dust
21 uplifting occurs in a source region when the surface wind speed exceeds a threshold velocity
22 (Gillette and Walker, 1977), which is a function of surface roughness elements, grain size, and
23 soil moisture (Marticorena and Bergametti, 1995; Wang et al., 2000). Fine soil particles that can
24 be transported over large distances are released by saltating coarse sand particles (Caquineau et
25 al., 1997). Soil morphology, mineralogy, and chemical composition define the abundance and
26 composition of airborne dust, however, not directly but through the series of complex fine-scale
27 non-linear processes.
28 From preliminary observations it is estimated that 5 to 6 major dust storms per year impact the
29 coastal region, depositing about 6 Mt of mineral dust into the Red Sea (Prakash et al., 2015).
30 Simulations and satellite observations suggest that the coastal dust contribution to the total
31 deposition flux into the Red Sea could be significant even during fair weather conditions (Jiang
32 et al., 2009). However, the mineralogy, physical properties, and chemical composition of dust
33 generated from the Red Sea coastal region remain uncertain. The coastal plain is a narrow highly
34 geographically and petrographically heterogeneous piedmont area, and existing soil databases do
35 not provide the have enough spatial resolution for the region to be to represent it adequately
36 described (Nickovic et al., 2012).
37 The importance of keeping track of dust mineralogy during the atmospheric transport was
38 recently recognized and implemented in the models (Perlwitz et al., 2015a, b). Equation (1)
39 relates the size-dependent soil dust properties with that emitted to~~in~~ the atmosphere, where dust
40 size-distribution and compositional characteristics are further adjusted as dust particles
41 atmospheric residence time depends on their particle size distribution and particle mass and
42 weights. The atmospheric dust size distribution and mineralogical/chemical composition defines
43 radiative, ecological, and health effects of dust. ~~To explain the connection between soil~~
44 ~~properties and airborne dust abundance and composition we~~ below discuss the physically-based
45 dust generation parameterizations currently used in the advanced modeling systems (Grell et al.,
46 2005; Zender et al., 2003). The vertical mass flux F_j ($\text{kg m}^{-2} \text{s}^{-1}$), of dust size component j , F_j (kg

1 $\text{m}^{-2}\text{s}^{-1}$), generated from the ground into the atmosphere can ~~ould~~ be ~~assessed~~ ~~calculated~~ ~~as~~
2 follows ~~in the following way~~:

$$3 F_j = TS f_m \alpha Q_s \sum_{i=1}^I M_{ij} \quad (1)$$

4 Where, T is a tuning constant for adjusting to different horizontal and temporal resolutions. The
5 parameter “ S ” is the erodibility factor that accounts for the susceptibility of a landscape to wind
6 erosion controlled by the non-erodible roughness elements and the erodibility of soils within the
7 erodible area of a landscape (Webb and Strong, 2011). This parameter S is often defined via the
8 so-called “source function” that accounts for the spatial distribution of dust source intensities
9 based on a variety of algorithms (Menut et al., 2013). The parameter f_m is a grid cell fraction of
10 exposed bare soil suitable for dust mobilization. The coefficient “ α ” is sandblasting mass
11 efficiency determined by the mass fraction of clay particles in the soil. The parameter Q_s is the
12 total horizontally saltation mass flux ($\text{kg m}^{-1} \text{s}^{-1}$), which is proportional to the third power of
13 friction velocity (u^*) when it exceeds a threshold velocity u^*_t (Oleson et al., 2010; Zender et al.,
14 2003). In dust emission models, the soil erodibility control is represented through the effects of
15 soil texture and moisture content on the threshold friction velocity u^*_t and the aerodynamic
16 roughness length f_r (Oleson et al., 2010; Webb and Strong, 2011). “ $M_{i,j}$ ” is the mass fraction of
17 each source mode i , carried in each transport bin j . The parameter “ S ” is the erodibility factor
18 that accounts for the susceptibility of a landscape to wind erosion controlled by the non-erodible
19 roughness elements and the erodibility of soils within the erodible area of a landscape (Webb and
20 Strong, 2011). In dust emission models, the soil erodibility control is represented through the
21 effects of soil texture and moisture content on the threshold friction velocity u^*_t and the
22 aerodynamic roughness length f_r (Oleson et al., 2010; Webb and Strong, 2011). The parameter S
23 is often defined via the so-called “source function” that accounts for the spatial distribution of
24 dust source intensities based on a variety of algorithms (Menut et al., 2013). The parameter Q_s is
25 the total horizontally saltation mass flux ($\text{kg m}^{-1} \text{s}^{-1}$), which is proportional to the third power of
26 friction velocity (u^*) when it exceeds a threshold velocity u^*_t (Oleson et al., 2010; Zender et al.,
27 2003).

28 Equation (1) relates the size-dependent soil dust properties with that emitted in the atmosphere,
29 where dust size distribution and compositional characteristics are further adjusted as dust
30 particles atmospheric residence time depends on their sizes and weights. The atmospheric dust
31 size distribution and mineralogical/chemical composition defines radiative, ecological, and
32 health effects of dust. The importance of keeping track of dust mineralogy during the
33 atmospheric transport was recently recognized and implemented in the models (Perlwitz et al.,
34 2015a, b). The sample area in this study lies within the approximately 60 – 70 km wide Tihāmah
35 coastal plain, comprised of the Tihāmat Asīr in the south and the Tihāmat Al-Hejaz to the north.
36 The plain is bounded by the Red Sea in the west, with the mountains of Midyan, Ash Shifa and
37 Asir forming an escarpment to the east (Edgell, 2006), with few breaks in the mountains in the
38 northwest. The mountains form a 1,000 – 3,000 m elevation Red Sea escarpment, comprised of
39 igneous, metamorphic and volcanic rocks of variable age, from Pre-cambrian (1,000 – 545
40 million years) to the less than 30 million years in age (Grainger, 2007). The Red Sea rift basin
41 itself is overlain by the much younger sediments of Quaternary age (< 2.6 million years).
42 Minerals previously found in continental soils from dust generation regions include quartz,
43 feldspars, calcite, dolomite, micas, chlorite, kaolinite, illite, smectite, palygorskite, mixed-layer
44 clays, iron oxides, gypsum, and halite (Pye, 1987; Scheuven and Kandler, 2014; Goudie,
45 2006; Engelbrecht and Moosmüller, 2014). Al-Farraj (2008) studied the soils from the Jazan
46 region of southern Saudi Arabia, identifying smectite, kaolinite and illite as the predominant clay

Field Code Changed

Field Code Changed

Field Code Changed

1 minerals, together with lesser amounts of chlorite, quartz and feldspars. Shadfan et al. (1984)
2 investigated mineralogical content and general characteristics of soils from some agricultural
3 areas in Saudi Arabia. They found carbonate, quartz and gypsum to be the main constituents of
4 the sand and silt fractions in soils of the eastern region, while quartz, carbonate and feldspars
5 dominate soils in the central region. The soils in the west contain mainly quartz, feldspars,
6 hornblende and mica. Palygorskite was found to be the main clay mineral in soils in the eastern
7 region, kaolinite in the central region, and kaolinite, smectite and mica in the western region.
8 Aba-Husayn et al. (1980) mineralogically analyzed soils from the southwestern region of Saudi
9 Arabia, along the mountainous Asir region between Mecca and Abha. They found major
10 amounts of quartz, feldspars and micaceous minerals in the silt fractions, with the clay-size
11 fractions of kaolinite, smectite, and vermiculite, with kaolinite in the well-drained highland
12 areas. Viani et al. (1983) studied fourteen soils from alluvial basins in the Wadi ad Dawasir, and
13 Wadi Najran areas of southwestern Saudi Arabia. Due to the fact that the alluvial clay-size
14 fractions were from weathered igneous rocks of the surrounding mountains, they were found to
15 be composed largely of smectite, mica, kaolinite, chlorite, palygorskite and vermiculite. ~~A
16 similar study on soils of the eastern region of Saudi Arabia (Lee et al., 1983) found smectite,
17 palygorskite, kaolinite, chlorite, mica and vermiculite in the clay-size fractions. The fallen dust
18 along the tracks of dust storms within major deserts in the world were collected and analyzed by
19 Al-Dousari and Al-Awadhi (2012). They showed that fallen dust from eastern zones
20 (Taklimakan, Gobi, and Australian deserts) are characterized by higher percentage of feldspar
21 and clay minerals in comparison to the western zones (Sahara and Arabian deserts) and western
22 Sahara desert dust is differentiated by the highest average quartz percentage (66%). Al-Dousari
23 and Al-Awadhi (2012) showed dust palls and sand dunes in Iraq to be composed of quartz,
24 feldspar, calcite, gypsum, dolomite and heavy minerals. Al-Dabbas et al. (2012) analyzed dust
25 samples over Iraq and showed the minerals as quartz (58.6%), feldspars (17.3%), calcite
26 (15.4%), and small amount of gypsum (5.5%). They also recognized clay minerals (chlorite,
27 illite, montmorillonite, palygorskite and kaolinite).~~
28 ~~The sample area in this study lies within the approximately 60–70 km wide Tihāmah coastal
29 plain, comprised of the Tihāmat Asir in the south and the Tihāmat Al-Hejaz to the north. The
30 plain is bounded by the Red Sea in the west, with the mountains of Midyan, Ash-Shifa and Asir
31 forming an escarpment to the east (Edgell, 2006), with few breaks in the mountains in the
32 northwest. The mountains form a 1,000–3,000 m elevation Red Sea escarpment, comprised of
33 igneous, metamorphic and volcanic rocks of variable age, from Pre-cambrian (1,000–545
34 million years) to the less than 30 million years in age (Grainger, 2007). The Red Sea rift basin
35 itself is overlain by the much younger sediments of Quaternary age (< 2.6 million years).~~

36 With the exception of the area around Jazan in the south, which is impacted by the Indian Ocean
37 monsoon, the Red Sea coastal region has a desert climate characterized by extreme heat,
38 reaching 39 °C during the summer days, with a drop in night-time temperatures of about 10 °C.
39 Although the extreme temperatures are moderated by the proximity of the Red Sea, in summer
40 the humidity is often 85% or higher during periods of the northwesterly *Shamal* winds. Annual
41 rainfall diminishes from an annual average of 133 mm at Jazan to 56 mm at Jeddah, and 24 mm
42 at Tabuk in the north. Vegetation is sparse, being restricted to semi-desert shrubs, and acacia
43 trees along the ephemeral rivers (wadis), providing forage for small herds of goats, sheep and
44 dromedary camels.

45 During infrequent but severe rainstorms, run-off from the escarpment along wadis often produce
46 flash floods. With such events, fine silt and clays are deposited on the coastal plain, which are

1 transformed into dust sources during dry and windy periods of the year. The resultant dust is
2 transported and deposited on the coastal plain and adjacent Red Sea by prevailing northwesterly
3 to southwesterly winds, with moderate breezes (wind speed >5.5 m/s) from the north
4 (<http://www.windfinder.com/weather-maps/report/saudi-arabia#6/22.999/34.980>).

5 6 **2. Objectives**

7 The assumption is that at least part of the dust in the ambient atmosphere in the coastal region is
8 from windblown and otherwise disturbed soils along the Red Sea coast. Jiang et al. (2009) and
9 Kalenderski et al. (2013) found that the coastal area emits about 5–6 Mt of dust annually. Due to
10 its close proximity, a significant portion of this dust is likely to be deposited to the Red Sea,
11 which could be comparable in amount to the estimated annual deposition rate from remote
12 sources during major dust storms (Prakash et al., 2015).

13 Due to the limited compositional information of soils along the Red Sea coastal region, t
14 his study aims to provide mineralogical, ~~and~~ chemical, and morphological information on
15 compositions of thirteen surface soils collected at four areas within the central part of the Red
16 Sea coastal plain of Saudi Arabia, (Fig. 1). ~~The dust hot spots are located within the narrow~~
17 ~~coastal region, and because of their proximity to the Red Sea, contribute to the dust/nutrient~~
18 ~~balance of the Sea, during both dusty and fair weather conditions. The coastal plains of the~~
19 ~~Arabian Peninsula along the Red Sea and Persian Gulf are among the most populated areas in~~
20 ~~this region hosting the major industrial and urban centers. Airborne dust profoundly affects~~
21 ~~human activities, marine and land ecosystems, climate, air quality, and human health. The~~
22 ~~observations suggest that the narrow Red Sea coastal belt is an important dust source region,~~
23 ~~augmented by the fine-scale sediment accumulations, scattered vegetation, and varying terrain.~~
24 Limited compositional information is available on soils along the Red Sea coastal region.
25 The present study examines soil mineralogical and chemical compositions, and individual
26 particle morphology from the samples taken at the hot spot areas. This information will help to
27 better quantify the ecological impacts, health effects, damage to property, and optical effects of
28 dust blown from these areas (Engelbrecht et al., 2009a, b; Weese and Abraham, 2009). The
29 mineralogical compositions of the soils tie into that of the parental rocks, weathering conditions
30 and time. This research will also complement soil and dust studies performed in the Arabian
31 Peninsula as well as globally (Engelbrecht and Moosmüller, 2014; Engelbrecht et al., 2009b).
32 Knowledge of the mineralogy of the soils will provide data on refractive indices, particle size
33 and shape parameters, which can be used to calibrate dust transport models, and help to assess
34 the impact of dust events on the coastal plain and the Red Sea.

35 **3. Sampling and analysis**

36 A total of thirteen samples were collected at four localities along the Red Sea coastal plain (Fig.
37 1). Three samples (S1–S3) collected at 25 km northeast of Mastorah near washland of Wadi
38 Hazahiz located 26 km from Red Sea. Samples (S4–S6) collected at 30 km east of Ar Rayis near
39 Ushash, which is a village in Al Madinah province located 32 km from Red Sea. Samples (S7–
40 S9) collected at 27 km north of Yanbu at washland of Wadi al Wazrah with an elevation of 158
41 m above sea level and located 30 km from Red Sea. Four samples (S10–S13) collected at 28 km
42 southwest of Mecca near Wadi An Numan located 45 km from Red Sea. The coordinates of the
43 sample sites are provided in Table 1. All thirteen samples can be classed as Leptosols (Regosols)
44 (<http://www.fao.org/ag/agl/agll/wrb/soilres.stm>).

1 ~~The assumption is that at least part of the dust in the ambient atmosphere in this coastal region is~~
2 ~~from windblown and otherwise disturbed soils along the Red Sea coast. Jiang et al. (2009) and~~
3 ~~Kalenderski et al. (2013) found that the coastal area emits about 5–6 Mt of dust annually. Due to~~
4 ~~its close proximity, a significant portion of this dust is likely to be deposited to the Red Sea,~~
5 ~~which could be comparable in amount to the estimated annual deposition rate from remote~~
6 ~~sources during major dust storms (Prakash et al., 2015).~~

7 The grab soil samples collected in the field were sieved to $D < 1$ mm to remove pebbles, plant
8 material and other ~~detritus~~~~unwanted artifacts~~. Where necessary, they were air-dried in the
9 laboratory, before being labeled, catalogued and stored in capped plastic bottles. Sub-sets of
10 these samples were screened to $D < 38$ μm for mineral analysis by X-ray powder diffraction
11 (XRD), chemical analysis, and Scanning Electron Microscopic (SEM) based individual particle
12 analysis. Further samples of 75 $\mu\text{m} < D < 125$ μm were sieved for mineralogical investigation by
13 optical microscopy, and $D < 600$ μm for Laser particle size analysis (LPSA).

14 Petrographic microscopy is particularly suited to the optical identification of mineral grains
15 larger than about 10 μm (Kerr, 1959). It remains a cost effective and accurate technique to obtain
16 mineralogical information which is otherwise difficult to obtain, e.g. the identification of
17 feldspars, amphiboles and pyroxenes. The 75 $\mu\text{m} < D < 125$ μm sieved soil fraction grains were
18 mounted in epoxy on a glass slide and ground to a thickness of approximately 30 μm , for
19 transmitted light optical microscopy. ~~Mineral optical properties such as texture, color,~~
20 ~~pleochroism, birefringence, relief, and twinning were used to identify silicate minerals and to~~
21 ~~estimate their abundance in the samples. Minerals with distinctive optical properties, including~~
22 ~~refractive indices, birefringence, extinction angles, pleochroism, and optical interference~~
23 ~~patterns, or those showing twinning, distinctive cleavage, and diagnostic extinction angles, can~~
24 ~~be readily be identified by optical microscopy (Kerr, 1959). Minerals readily identified in these~~
25 ~~samples by this method include quartz, various feldspars, amphiboles, pyroxenes, micas and~~
26 ~~carbonates. However, depending on the mineral type, particles < 10 μm in diameter are often~~
27 ~~difficult to identify by this method, including clay minerals and other layered silicates. The~~
28 ~~method requires the samples preferably to be mounted in epoxy as a polished thin section. The~~
29 ~~method is biased towards easily identifiable and coarser minerals, especially those with twinning~~
30 ~~such as feldspars, and showing color and pleochroism such as hornblende and biotite. The~~
31 ~~method, although one of the most practical for qualitative mineral analysis, does require~~
32 ~~mineralogical expertise.~~

33 ~~Optical properties such as scattering, absorption and refractive indices vary, depending on the~~
34 ~~mineralogical content of the dust in the atmosphere.~~

35 X-ray diffraction (XRD) is a non-destructive technique for characterization of minerals,
36 ~~including quartz, feldspars, calcite, dolomite, clay minerals, and iron oxides, particularly for the~~
37 ~~fine soil and dust fractions~~. Dust reactivity in the seawater as well as optical properties depend
38 on their mineralogy, e.g. carbonates and some silicates are generally more soluble in water than
39 for example feldspars, amphiboles, pyroxenes or quartz. A Bruker D8[®] X-ray powder diffraction
40 (XRD) system was used to analyze the mineral content of the soil samples. The diffractometer
41 was operated at 40 kV and 40 mA, with Cu K α radiation, scanning over a range of 4° to 50° 2θ .
42 The Bruker Topas[®] software and relative intensity ratios were applied for semi-quantitative XRD
43 analyses of the $D < 38$ μm screened dust samples (Rietveld, 1969; Chung, 1974; Esteve et al.,
44 1997; Caquineau et al., 1997; Sturges et al., 1989). Powder XRD is particularly suited for fine-
45 grained crystalline mineral mixtures, < 10 μm in diameter. The procedure measures the

Formatted: Font: (Default) Times New Roman, 12 pt,
Font color: Auto

1 crystallinity of a sample, i.e. excludes amorphous phases such as clay-like colloids (!!!
2 INVALID CITATION !!! (Formenti et al., 2011;Leinen et al., 1994;Engelbrecht et al.,
3 2016;Kandler et al., 2009)), partly crystalline layered silicates such as some clays, and
4 hydroxides. If an amorphous phase is present, it will not be fingerprinted by XRD. The
5 assessment of mineral content of a powder sample by the relative intensity ratio (RIR) method
6 suggested by Chung (1974), and as applied in our measurements, does not account for
7 amorphous content.

Formatted: Font: (Default) Times New Roman, 12 pt,
Font color: Auto

Formatted: Font: (Default) Times New Roman, 12 pt,
Font color: Auto

Formatted: Font: (Default) Times New Roman, 12 pt,
Font color: Auto

Formatted: Font: (Default) Times New Roman, 12 pt,
Font color: Auto

8 Laser particle size analysis (LPSA) was performed on the thirteen soil samples. The LPSA
9 system measures the size-class fractions of a soil or sediment sample in an aqueous suspension,
10 based on the principle that light scatters at angles inversely proportional to, and with intensity
11 directly proportional to particle size (Gee and Or, 2002). ~~Dust emission rates from soils and sites~~
12 ~~of airborne particles strongly depend on the soil particle size distributions. The optical properties~~
13 ~~of airborne particles, such as scattering and absorption, depend on their particle sizes.~~The grab
14 samples were sieved to $D < 600 \mu\text{m}$ before being introduced to the laser analyzer (Micromeritics
15 Saturn DigiSizer 5200[®]) in an aqueous medium solution of 0.005% surfactant (sodium
16 metaphosphate). The suspensions were internally dispersed by applying ultra-sonication, and
17 circulated through the path of the laser light beam. The measured size-class fractions were
18 grouped as clay ($D < 2 \mu\text{m}$), silt ($2 \mu\text{m} < D < 62.5 \mu\text{m}$) and sand ($62.5 \mu\text{m} < D < 600 \mu\text{m}$),
19 (Engelbrecht et al., 2012). This analytical method disperses soil aggregates which are potential
20 dust particles, so shifting the particle size distribution curves towards the smaller particle sizes.
21 This may introduce a bias into the actual size distribution of wind generated dust particles in the
22 field.

Field Code Changed

Formatted: Font: (Default) Times New Roman, 12 pt,
Font color: Auto

23 The $D < 38 \mu\text{m}$ sieved samples were chemically analyzed for elemental composition by
24 Inductively Coupled Plasma Optical Emission Spectrometry (ICP-OES), and their water soluble
25 ions by Ion Chromatography (IC). For ICP-OES, splits of 0.1g of each of the samples were
26 digested in a 1:3:1 mixture of concentrated hydrofluoric acid (HF), hydrochloric acid (HCl) and
27 nitric acid (HNO_3), in a microwave oven (Milestone Ethos1[®]) operated at a temperature up to
28 195°C for 15 minutes. The solutions were diluted from 25 ml to 250 ml before being analyzed
29 on a ICP-OES (Varian 720-ES[®]), for sodium (Na), magnesium (Mg), aluminum (Al), silicon
30 (Si), phosphorus (P), sulfur (S), potassium (K), calcium (Ca), titanium (Ti), vanadium (V),
31 chromium (Cr), manganese (Mn), iron (Fe), cobalt (Co), nickel (Ni), copper (Cu), zinc (Zn),
32 strontium (Sr), cadmium (Cd), barium (Ba) and lead (Pb). The accuracy of the analyses was
33 monitored by analyzing the National Institute of Standards and Technology (NIST) standard
34 reference material 1646a with each batch of soil samples. The elemental composition of dust per
35 se does not provide adequate information on its mineral content. However, with a priori
36 knowledge of the mineral composition of the samples, from optical and XRD measurements,
37 “normative” mineral compositions can be calculated. This provides a method for inter-comparing
38 chemically analyzed samples with each other.

39 Further splits (approx. 0.01 g) of the $D < 38 \mu\text{m}$ sieved samples were sonicated in 15 ml of de-
40 ionized distilled water, the suspension left to settle overnight, and the extractions analyzed by IC
41 (DIONEX ICS-3000[®]). The water soluble cations of sodium (Na^+), potassium (K^+), calcium
42 (Ca^{2+}) and magnesium (Mg^{2+}), and anions of sulfate (SO_4^{2-}), chloride (Cl^-), phosphate (PO_4^{3-})
43 and nitrate (NO_3^-) were analyzed by this method.

44 Electron microscopy provides information on the individual particle size, shape, chemical
45 composition, and mineralogy of micron-size particles, important for determining the optical
46 parameters for modeling of dust (Moosmüller et al., 2012). The individual particle chemistry,

1 especially of the soluble minerals such as carbonates, is often of importance in medical geology
2 and to marine life. The Scanning Electron Microscope (SEM) based individual particle analysis
3 was performed on the $D < 38 \mu\text{m}$ sieved sample splits. A dual approach was followed, the first
4 being the computer controlled scanning electron microscopy (CCSEM) and the second,
5 secondary electron imaging by high resolution scanning electron microscopy (SEM). For each
6 sample, a portion of soil was suspended in isopropanol and dispersed by sonication. The
7 suspension was vacuum filtered onto a $0.2 \mu\text{m}$ pore size polycarbonate substrate. A section of the
8 substrate was mounted onto a metal SEM stub with colloidal graphite adhesive. The sample
9 mounts were sputter-coated with carbon to dissipate the negative charge induced on the sample
10 by the electron beam. The automated CCSEM analysis was conducted on a Tescan MIRA 3[®]
11 field emission scanning electron microscope (FE-SEM). The CCSEM analysis was performed by
12 rastering the electron beam over the sample while monitoring the resultant combined
13 backscattered electron (BE) and secondary electron (SE) signals. The BE intensities were applied
14 to set grayscale levels, to distinguish particles of interest from background. The system was
15 configured to automatically measure the size and the elemental composition for about 2,000
16 individual particles of $0.5 > D > 38 \mu\text{m}$ sizes. Individual particles were classified into particle
17 types according to their elemental compositions. A digital image was acquired of each particle
18 for measurement, and stored for subsequent review. Size measurements were based on diameters
19 obtained from the projected area of each particle, by tracing their outer edges. Compositional
20 information was determined through collection and processing of characteristic X-rays by energy
21 dispersive spectroscopy (EDS) using a silicon drift detector (SDD). The elements identified in
22 the spectrum were processed to obtain their relative concentrations. The particles were grouped
23 into “bins” by their particle size and chemical ratios. From the chemical measurements, and a
24 priori knowledge of the sample mineralogy (from optical microscopy and XRD), the mineralogy
25 of individual particles can often be inferred, e.g. Si particles being quartz, Ca particles being
26 calcite, Ca plus S particles being gypsum. Due to the attenuation of the electron beam as it
27 impinges the particle surface and loss of energy, the analysis is physically limited to an electron
28 interaction volume of 2–5 μm below the mineral surface, depending on the primary beam voltage
29 and the mineral density (Goldstein et al., 2003). Most of the investigated mineral dust particles
30 have coatings of clay minerals and oxides, which results in an overestimation of the amounts of
31 these minerals when analyzed by CCSEM (Engelbrecht et al., 2009a; Engelbrecht et al.,
32 2016; Engelbrecht et al., 2009b).
33 The field emission electron source allows for high magnifications and sharp secondary electron
34 images (SEI). This technique allows for the detailed study of particle shape, surface features, and
35 chemical compositions. Approximately five SEI’s with energy dispersive spectra (EDS) for each
36 of the thirteen samples were collected. Fig. B3 (Appendix B) shows SEM secondary electron
37 images and EDS spectra of $D < 38 \mu\text{m}$ soil particles from the sampling site.

38 4. Results

39 4.1 Particle Size Analysis

40 Particle volume size plots of the $D < 600 \mu\text{m}$ sieved samples are listed in Table 2 and graphically
41 presented in Fig. 2. ~~The~~ thirteen soils are composed of on average close to 89% sand
42 fractions. Also, the silt makes up approximately 10% and the clay on average less than 1.5% of
43 the sample volume.

44 Field and laboratory measurements on dust from the western U.S.A. (Engelbrecht et al., 2012)
45 showed that dust emissions are largely controlled by their soil particle size distributions (Kok,

1 2011a, b). It was established that surface soils with a silt content of greater than about 50% and a
2 clay content of less than about 10%, i.e. samples in the “silt loam” field (Fig. 2) have the greatest
3 potential to become re-suspended in the air and to generate airborne mineral dust. This particle
4 size criterion provides an important measure for whether a site or region has the potential to be a
5 significant dust source (Greely and Iversen, 1985). These include soils from previously identified
6 dust sources such as Bodélé Depression (Washington et al., 2003), loess along the Danube River
7 valley, Kuwait, China (Engelbrecht and Moosmüller, 2014), silt deposits collected on
8 Fuerteventura Island assumed to contain dust from the western Sahara (Menéndez et al., 2014),
9 as well as one diatomaceous silt sample from Reno, USA. Besides the particle size distribution it
10 was shown that moisture content and surface roughness play important roles in the saltation and
11 de-segregation of soil particles (Marticorena, 2014). Judging from their particle size distributions
12 alone, soil samples collected from the coastal zone of Saudi Arabia are not considered to contain
13 enough silt-size particles to be efficient emitters of dust. However, the satellite images show that
14 these coastal dust sources are activated quite frequently.

15 **4.2 Optical microscopy**

16 Mineralogical investigation by optical microscopy of three $75 \mu\text{m} < D < 125 \mu\text{m}$ sieved samples
17 showed them to consist of partially weathered angular mineral grains in sediments probably
18 eroded from the Pre-Cambrian basement and Tertiary volcanic rocks of the Arabian Shield,
19 approximately 50 km to the east of the Red Sea coastline (Edgell, 2006). The major minerals
20 identified in this size range are feldspar (mainly plagioclase), quartz, pyroxene (aegerine-augite),
21 amphibole, and mica (biotite, muscovite). Lesser amounts of potassium feldspar (orthoclase,
22 microcline), carbonates (calcite, dolomite), chlorite, epidote and oxides were identified by
23 optical microscopy.

24 **4.3 XRD mineral analysis**

25 XRD analysis of the thirteen, $D_{<38 \mu\text{m}}$ sieved samples from the Red Sea coastal plain (Fig. 3)
26 confirmed variable ~~mass percentages amounts~~ of quartz (19 – 44%) and feldspars (plagioclase,
27 K-feldspar) (31 – 48%), ~~as well as of with variable amounts of~~ amphibole (and pyroxene) (4 –
28 31%), lesser amounts of calcite (0.4 – 6.2%), dolomite (1.9 – 6.6%), clays and chlorite (smectite,
29 illite, palygorskite, kaolinite) (3.3 – 8.3%), with traces of gypsum (0 – 0.6%) and halite (0.2 –
30 4.8%). For this and other localities, the mineralogy resembles that of the igneous and
31 metamorphic rocks of the adjacent mountainous escarpment and Arabian Shield (Edgell, 2006).
32 The average amphibole (plus pyroxene) content for the four samples taken at the southernmost
33 locality (Fig. 1, S10 – S13) is substantially higher than for the nine samples taken at the other
34 three localities (Fig. 1, S1 – S9), being approximately 26% for the former and 11% for the later.
35 This can be attributed to differences in the mineral composition of the Arabian Shield rocks,
36 distance of the sampling sites from the source regions, and the extent of weathering in the
37 surface soils.

38 **4.4 Chemistry (ICP-OES and IC)**

39 Chemical analysis of the $D < 38 \mu\text{m}$ sieved bulk samples by ICP-OES and IC are presented in
40 Tables ~~AE1&AE2~~ (appendix ~~AE~~) and a plot of the major elements expressed as oxides, shown
41 in Fig 4. The soils are of consistent chemical compositions throughout the sampled region.
42 The sedimentary samples all contain major ~~mass~~ percentages of SiO_2 , varying between 63% and
43 78% in the thirteen samples, mostly as the mineral quartz, and lesser ~~mass percentages amounts~~
44 of Al_2O_3 , CaO , Na_2O , and K_2O , in plagioclase and potassium feldspars. SiO_2 together with

1 Al₂O₃, Fe₂O₃, TiO₂, MnO, MgO, and some K₂O is also contained in the previously identified
2 amphiboles, clays and micas. Small amounts of CaO (0.9 – 1.7%) are contained in gypsum and
3 calcite, and together with MgO (2.3 – 3.1%) in dolomite.

4 The water soluble ions account for a small percentage of the total mass of the soils, varying
5 between 0.1% and 0.7% for the total cations, and 0.03% and 0.8% for the total anions. These
6 account primarily for calcite and dolomite (~ 0.3%), and gypsum (~ 0.2%), with lesser amounts
7 of halite and other chlorides from sea salt. This unexpectedly low concentration of halite and
8 other soluble salts in the soils of the coastal plains can be ascribed to the fact that all the samples
9 were collected at distances varying between 21 and 42 km from the Red Sea coast, and the
10 absence of local playas or other saline soils close to the four sampling areas. It is also expected
11 that the salts had been leached from the soil samples collected from surface. Also of importance
12 to dust borne nutrients likely to be deposited in the Red Sea is the low concentration of water
13 soluble PO₄³⁻ (avg. 0.003 %) in comparison to the total P₂O₅ (avg. 0.4%) in the soils. The
14 phosphorus is largely bound in the low soluble mineral apatite, commonly found in the
15 sediments throughout the Arabian Peninsula.

16 The Fe/Al mass ratios for the suite of 13 samples from the Red Sea coastal plain vary between
17 1.26 and 3.59, with a geometric mean 2.41 (Appendix A). These measurements partly overlap
18 with the Fe/Al ratios of 0.53 – 1.71 measured for dust samples from the Bodélé Depression in
19 Chad (Bristow et al., 2010), and included in the range of 0.41 – 3.78 for 136 re-suspended soil
20 samples from global dust sources (Engelbrecht et al., 2016). In contrast, soil samples collected
21 from ferricretes along the southern Sahel in northern Africa have Fe/Al ratios in the range of
22 2.95 to 3.43 (Roquin et al., 1990).

23 4.5 SEM chemical analysis

24 Approximately 2000 individual dust particles per sample in the 0.5 – 38 µm size range were
25 analyzed automatically by CCSEM, for chemical composition, particle morphology and size.
26 The particles were classed into 14 bins as per their chemical compositions. Mineral labels were
27 assigned to these chemical bins, e.g. Fe-rich as hematite (Fe₂O₃) (also possibly goethite,
28 magnetite or ferrihydrite), Ca-S rich as gypsum (CaSO₄·2H₂O), Ca-Mg rich as dolomite
29 (CaMg(CO₃)₂), Ca rich as calcite (CaCO₃), Ca-Al-Si rich as anorthite (CaAl₂Si₂O₈), Na-Al-Si
30 rich as albite (NaAlSi₃O₈), K-Al-Si rich as K-feldspar (KAlSi₃O₈), and Si-rich as quartz (SiO₂).
31 The CCSEM results for the 0.5 – 38 µm analyzed set as well as the 0.5 – 2.5 µm (fine) subset are
32 presented in Fig. 5 and 6.

33 For the total data set, the samples in the 0.5 – 38 µm size range contain by mass about 0.1 –
34 10.2% Si (quartz), 5 – 54% feldspar, 45 – 72% clay minerals, as major components with lesser
35 amounts of calcite, dolomite, gypsum, and iron oxides. The clay minerals can occur as individual
36 minerals but largely as coatings on other silicates (Engelbrecht et al., 2009a). The 0.5 – 38 µm
37 set shows a substantial variability in chemical composition, but no distinct differences between
38 the samples within the four localities. The 0.5 – 2.5 µm (fine) subsets of the three samples (S7,
39 S8, and S9) are different from the others in their higher Fe-rich (goethite, hematite) and carbon
40 (carbonates) components, and corresponding smaller amounts of clay (Fig. 6). This can be
41 ascribed to a local difference in the mineralogical composition of the undifferentiated source
42 rocks (Edgell, 2006), as well as weathering conditions.

43 The size and shapes of the thirteen, D < 38 µm sieved samples are given in Tables A1 & A2
44 (appendix A), with the size distributions graphically displayed in Fig. B1 & B2 (appendix B)
45 Fig. 7 shows the average particle size distributions, as well as size and shape (aspect ratio)
46 statistics for D < 38 µm sieved samples, as measured by scanning electron microscopy

1 ~~(CCSEM)~~–For individual samples, the particle sizes are approximately log normally distributed
2 (skewness = 2.3 – 5.5), often showing a slight bimodality, with a small maximum (approx. 12
3 μm) on the high end of the distributions. The latter can be ascribed to harder, larger silt size
4 particles of quartz and feldspars. The greatest number of particles are tightly clustered about their
5 mean diameters, resulting in high but variable kurtosis values (4.6 – 44.0). The geometric mean
6 diameters for the particles lie in the small range of 2.1 to 3.7 μm , implying similar mineralogy
7 and hardness. ~~and containing sheet silicates such as clays, chlorites, and micas.~~ The mean
8 aspect ratios of the particles also fall in a tight range of 1.40 to 1.48, with a mean value of 1.43.

9 **5. Summary Discussion and Conclusions**

10 ~~Mineral dust generated by wind erosion of soils is the major contributor to global aerosol mass
11 loading and column optical thickness. It is especially abundant in the desert and semi-desert
12 regions. Dust affects marine life providing nutrients to the marine environment and controlling
13 incoming solar and terrestrial radiation. Soils in arid regions are most susceptible to wind erosion,
14 where particles are only loosely bound to the surface by the low soil moisture. Dust uplifting
15 occurs in a source region when the surface wind speed exceeds a threshold velocity (Gillette and
16 Walker, 1977), which is a function of surface roughness elements, grain size, and soil moisture
17 (Marticorena and Bergametti, 1995; Wang et al., 2000). Fine soil particles that can be transported
18 over large distances are released by saltating coarse sand particles (Caquineau et al., 1997). So
19 soil morphology, mineralogy, and chemical composition define the abundance and composition
20 of airborne dust, however, not directly but through the series of complex fine-scale non-linear
21 processes.~~

22 The impact of soil dust from natural and anthropogenic sources on climate and air quality has
23 been recognized on a global scale (Sokolik and Toon, 1996; Tegen and Fung, 1995). However,
24 the regional fine-scale processes of mineral dust emissions and their effect on the environmental
25 processes and human health are poorly quantified in the study region because the spatial
26 distribution of detailed mineralogical, physical and chemical properties of the surface soils at
27 coastal dust source regions (“hot-spots”) were previously not available.

28 The application of a range of techniques for the analysis of properties of soil samples allows for
29 a better understanding of mineral dust. However, the different analytical methods often provide
30 different results, as seen by comparing the XRD, electron microscopy and chemistry of the soils.
31 In this study, the results from the XRD analysis gives a quartz percentage of between about 19
32 and 44 % and sheet silicates (clays, micas) of between 3 and about 8%. In contrast, the single
33 particle analysis by CCSEM gives a quartz fraction of only up to about 10%, whereas the sheet
34 silicates always have the largest mineral percentage, of up to about 72%. This can lead to
35 ambiguity in the interpretation of the mineralogical composition of the samples. This is evident
36 even where the mineral composition is investigated for the same size range, i.e. < 38 μm particle
37 diameter. Biases in XRD results can be related to the presence of partly amorphous sheet
38 silicates with poor crystallization (Leinen et al., 1994; Formenti et al., 2008; Kandler et al.,
39 2009; Engelbrecht et al., 2016) and a subsequent overestimation of the quartz fractions. Knowing
40 the answers to such questions would be necessary for properly using the data to constrain or
41 evaluate simulations with dust models. Similarly, the individual particle analysis by CCSEM
42 provides an overestimation of the clay fraction which can be attributed to surface coatings on the
43 quartz and its underestimation (Engelbrecht et al., 2009a, b; Engelbrecht et al., 2016). What is of
44 importance when considering the application of these results in models, health studies, and
45 remote sensing, is not only the mineralogical composition of the dust, but also their
46 mineralogical interrelationships such as mineral clusters, mineral coatings, and intergrowths.

1 From satellite images we identified four Red Sea coastal areas from which dust was frequently
2 emitted (Jiang et al., 2009;Kalenderski et al., 2013). The thirteen soil grab samples were
3 collected from these areas for analysis and their mineralogy, chemical composition and particle
4 size distributions were studied. We found that the Red Sea coastal samples collected in this study
5 contain major components of quartz and feldspar (plagioclase, orthoclase), as well as lesser but
6 variable amounts of amphibole (hornblende), pyroxene (aegerine-augite), carbonate (calcite,
7 dolomite), clays (illite, palygorskite, kaolinite, smectite), and micas (muscovite, biotite), with
8 traces of gypsum, halite, chlorite, epidote and oxides. The range of identified minerals is ascribed
9 to the variety of igneous and metamorphic provenance rocks along the escarpment to the east of
10 the Red Sea coastal plain (Edgell, 2006). Similarly high fractions of quartz and feldspars were
11 reported for Kuwait (Engelbrecht et al., 2009b) and to a lesser extent for Tallil, Tikrit and Taji in
12 Iraq. The samples from the Red Sea coastal region of Saudi Arabia differ substantially from
13 those from Afghanistan, Qatar, UAE, Iraq and Kuwait in that they contain substantially less
14 calcite. They also contain ~~much less~~ dolomite than the sample from Al Asad in Iraq. These
15 deviations in composition could be ascribed to differences in provenance and geology. The
16 coastal plain is bounded by the Red Sea in the west, with the mountains of Midyan, Ash Shifa
17 and Asir forming an escarpment to the east and the provenance for water borne sediments to the
18 wadis along the coastal plain. Since the igneous and metamorphic source rocks are composed of
19 a wide range of minerals including quartz, feldspars, amphiboles, pyroxenes, and micas, it can be
20 assumed that the partially weathered sediments transported to the coastal plain during flash
21 floods will contain similar minerals, which can in turn be suspended as mineral dust. In contrast
22 the samples collected in Kuwait, Iraq and Afghanistan are from extensive flat lying areas, and ~~to~~
23 ~~some extent~~ contain minerals such as quartz, calcite, and dolomite from local sedimentary rocks.
24 Djibouti lies along the African Rift Valley along the west coast of the Gulf of Aden and close to
25 igneous and metamorphic rock formations of the Nubian Plate, separated from the
26 petrographically similar Arabian Plate by the Red Sea, both regions containing rock formations
27 with substantial amounts of pyroxene, amphibole, and plagioclase. This at least in part explains
28 the similarity of soils and dust at Djibouti to those along the coastal plain of Saudi Arabia, The
29 mineralogical content of the soils was found to be closely related to the regional geology.
30 Particle size analysis on the sampled soils showed them to contain too much sand and too little
31 silt to be considered major globally important sources of airborne dust, compared to renowned
32 global sources such as the Bodélé Depression, and silt covered regions of northwest U.S.A.
33 (Engelbrecht et al., 2012;Engelbrecht and Moosmüller, 2014). The low silt content in the
34 investigated samples suggests that the dust plume generated from the Red Sea coastal region is
35 enriched by the coarse dust fraction that deposits quickly. As seen from atmospheric
36 observations, the coastal region is the origin of frequent dust plumes over the Red Sea, probably
37 due to frequent strong wind gusts. These mostly coarse dusts could not be transported the vast
38 distances to the Red Sea and directly deposited there, affecting marine life. Our analysis ~~has~~
39 revealed that the samples contain compounds of nitrogen, phosphorus and iron, that are essential
40 nutrients to marine life (Guerzoni et al., 1997;Migon et al., 2001). The integration of analytical
41 information on dust mineralogy and mineralogical interrelationships, chemistry, and physical
42 properties of soils provides a better understanding of their potential impact on the communities
43 living along the Red Sea (Edgell, 2006;UCAR/NCAR, 2003;Washington et al., 2003). The
44 results from this study can also provide improvements to the input of climate forecasting and
45 dust emission models. The thirteen chemical source profiles will complement those of soil

1 samples collected in other regions of the Middle East (Engelbrecht et al., 2009b), in source
2 attribution studies.

3 -Analytical methods developed in this phase of the dust program will be applied for analysis of
4 dust samples deposited from the atmosphere for aerosol characterization studies in the Red Sea
5 coastal region. These will allow further assessing the impact of elevated dust concentrations on
6 regional climate, marine ecology, air quality, and health.

7 **Data Availability**

8 The mineralogical and chemical data from this study are available upon request from Georgiy
9 Stenchikov (Georgiy.Stenchikov@kaust.edu.sa).

10 **Author Contributions**

11 Georgiy Stenchikov formulated the problem, designed the research project, and supported
12 experimental activities; Johan Engelbrecht advised on aerosol analysis and instrumentation;
13 Weichun Tao defined the dust source areas using satellite observations; Jish Prakash conducted
14 measurements, analysed and combined results; Tahir Yapici and Bashir Warsama helped with
15 instrumentation in the Kaust Core Lab. Prakash, Engelbrecht, and Stenchikov wrote different
16 parts of the paper.

17 **Acknowledgements**

18 This research, including the chemical and mineralogical analysis is supported by internal funding
19 from the King Abdullah University of Science and Technology (KAUST). For chemical
20 analyses, this research used the resources of the KAUST core lab. We acknowledge the
21 contribution from the collaborating laboratories of the RJ Lee Group and Desert Research
22 Institute.

23

1 References

- 2 Aba-Husayn, M. M., Dixon, J. B., and Lee, S. Y.: Mineralogy of Saudi Arabian Soils:
3 Southwestern Region, Soil Sci. Soc. Am. J., 44, 643-649,
4 10.2136/sssaj1980.03615995004400030043x, 1980.
- 5 Acosta, F., Ngugi, D. K., and Stingl, U.: Diversity of picoeukaryotes at an oligotrophic site off the
6 Northeastern Red Sea Coast, Aquat. Biosyst., 9, 10.1186/2046-9063-9-16, 2013.
- 7 ~~Al-Dabbas, M. A., Ayad Abbas, M., and Al-Khafaji, R. M.: Dust storms loads analyses Iraq,
8 Arabian J. Geosci., 5, 121-131, 10.1007/s12517-010-0181-7, 2012.~~
- 9 ~~Al-Dousari, A., and Al-Awadhi, J.: Dust fallout in northern Kuwait, major sources and
10 characteristics, Kuwait J. Sci. Eng., 39(2A), 171-187, 2012.~~
- 11 Al-Farraj, A. S.: The mineralogy of clay fractions in the soils of the southern region of Jazan, Saudi
12 Arabia, J. Agron., 7, 115-126, 2008.
- 13 Bennett, C. M., McKendry, I. G., Kelly, S., Denike, K., and Koch, T.: Impact of the 1998 Gobi
14 dust event on hospital admissions in the Lower Fraser Valley, British Columbia, Sci. Total
15 Environ., 366, 918-925, 10.1016/j.scitotenv.2005.12.025, 2006.
- 16 Bennion, P., Hubbard, R., O'Hara, S., Wiggs, G., Wegerdt, J., Lewis, S., Small, I., van der Meer,
17 J., and Upshur, R.: The impact of airborne dust on respiratory health in children living in the Aral
18 Sea region, Int. J. Epidemiol., 36, 1103-1110, 10.1093/ije/dym195, 2007.
- 19 Brindley, H., Osipov, S., Bantges, R., Smirnov, A., Banks, J., Levy, R., Jish Prakash, P., and
20 Stenichkov, G.: An assessment of the quality of aerosol retrievals over the Red Sea and evaluation
21 of the climatological cloud-free dust direct radiative effect in the region, J. Geophys. Res.: Atmos.,
22 120, 2015JD023282, 10.1002/2015JD023282, 2015.
- 23 \mp
- 24
- 25 Bristow, C. S., Hudson-Edwards, K. A., and Chappell, A.: Fertilizing the Amazon and equatorial
26 Atlantic with West African dust, Geophysical Research Letter, 37, L14807,
27 doi:10.1029/2010GL043486, 2010.
- 28
- 29
- 30 Buseck, P. R., Jacob, D. J., Pósfai, M., Li, J., and Anderson, J. R.: Minerals in the air: An
31 environmental perspective, International Geology Review, Symposium, Stanford, California,
32 1999.
- 33 Caquineau, S., Magonthier, M.-C., Gaudichet, A., and Gomes, L.: An improved procedure for the
34 X-ray diffraction analysis of low-mass atmospheric dust samples, Eur. J. Mineral., 9, 157-166,
35 1997.
- 36 Chung, F. H.: Quantitative interpretation of X-ray diffraction patterns of mixtures. I. Matrix-
37 flushing method for quantitative multicomponent analysis, J. Appl. Crystallogr., 7, 519-525,
38 doi:10.1107/S0021889874010375 1974.
- 39 De Longueville, F., Hountondji, Y. C., Henry, S., and Ozer, P.: What do we know about effects of
40 desert dust on air quality and human health in West Africa compared to other regions?, Sci. Total
41 Environ., 409, 1-8, 2010.
- 42 Edgell, H. S.: Arabian Deserts. Nature, Origin and Evolution, Springer, Dordrecht, Netherlands,
43 592 pp., 2006.
- 44 Engelbrecht, J. P., McDonald, E. V., Gillies, J. A., Jayanty, R. K. M., Casuccio, G., and Gertler,
45 A. W.: Characterizing mineral dusts and other aerosols from the Middle East – Part 1: Ambient
46 sampling, Inhalation Toxicol., 21, 297-326, 2009a.

1 Engelbrecht, J. P., McDonald, E. V., Gillies, J. A., Jayanty, R. K. M., Casuccio, G., and Gertler,
2 A. W.: Characterizing mineral dusts and other aerosols from the Middle East – Part 2: Grab
3 samples and re-suspensions, *Inhalation Toxicol.*, 21, 327-336, 2009b.

4 Engelbrecht, J. P., Gillies, J. A., Etyemezian, V., Kuhns, H., Baker, S. E., Zhu, D., Nikolich, G.,
5 and Kohl, S. D.: Controls on mineral dust emissions at four arid locations in the western USA,
6 *Aeolian Res.*, 6, 41-54, 2012.

7 Engelbrecht, J. P., and Moosmüller, H.: Mobile Aerosol Monitoring System for Department of
8 Defense - Continuous Aerosol and Aerosol Optics Measurement in Theater, U.S. Army Medical
9 Research and Materiel Command, Fort Detrick, Maryland Report W81XWH-11-2-0220, 1-229,
10 2014.

11 [Engelbrecht, J. P., Moosmüller, H., Pincock, S., Jayanty, R. M., Lersch, T., and Casuccio, G.:
12 Technical Note: Mineralogical, chemical, morphological, and optical interrelationships of mineral
13 dust re-suspensions, *Atmospheric Chemistry and Physics, Discussion*, 10.5194/acp-2016-286,
14 2016.](#)

15 Esteve, V., Rius, J., Ochando, L. E., and Amigó, J. M.: Quantitative x-ray diffraction phase
16 analysis of coarse airborne particulate collected by cascade impactor sampling, *Atmos. Env.*, 31,
17 3963-3967, doi:10.1016/S1352-2310(97)00257-4 1997.

18 [Formenti, P., Rajot, J. L., Desboeufs, K., Said, F., Grand, N., Chevaillier, S., and Schmechtig, C.:
19 Airborne observations of mineral dust over western Africa in the summer Monsoon season: spatial
20 and vertical variability of physico-chemical and optical properties, *Atmospheric Chemistry and
21 Physics*, 11, 6387–6410, 10.5194/acp-11-6387-2011, 2011.](#)

22 Fryrear, D. W.: Long-term effect of erosion and cropping on soil productivity, Spec. Pap. - Geol.
23 Soc. Am., 186, 253-260, 10.1130/SPE186-p253, 1981.

24 Gee, G. W., and Or, D.: Particle-size analysis, in: *Methods of Soil Analysis: Part 4–Physical
25 Methods*, No. 5, edited by: Dane, J. H., and Topp, G. C., Soil Science Society of America,
26 Madison, WI., 255-293, 2002.

27 Gillette, D. A., and Walker, T. R.: Characteristics of airborne particles produced by wind erosion
28 of sandy soil, High Plains of West Texas, *Soil Sci.*, 123, 97-110, 1977.

29 Goudie, A. S., and Middleton, N.J.: *Desert Dust in the Global System*, Springer, 287 pp., 2006.

30 Grainger, D.: *The Geological Evolution of Saudi Arabia, a Voyage through Space and Time* Saudi
31 Geological Survey, 2007.

32 Greely, R., and Iversen, J. D.: *Wind as a geological process on Earth, Mars, and Venus*, Cambridge
33 University Press, Cambridge, 333 pp., 1985.

34 Grell, G., Peckham, S. E., Schmitz, R., A., M. S., Frost, G., Skamarock, W. C., and Eder, B.: Fully
35 coupled "online" chemistry within the WRF Model, *Atmos. Env.*, 39, 6957-6975, 2005.

36 Guerzoni, S., Molinaroli, E., and Chester, R.: Saharan dust inputs to the western Mediterranean
37 Sea: depositional patterns, geochemistry and sedimentological implications, *Deep Sea Res., Part
38 II*, 44, 631–654, 1997.

39 Hagen, L. J., and Woodruff, N. P.: Air pollution from dust storms in the Great Plains, *Atmos. Env.*,
40 7, 323-332, 1973.

41 Haywood, J., and Boucher, O.: Estimates of the direct and indirect radiative forcing due to
42 tropospheric aerosols: A review, *Rev. Geophys.*, 38, 513-543, 10.1029/1999RG000078, 2000.

43 Hsu, N. C., Tsay, S. C., King, M. D., and Herman, J. R.: Aerosol properties over bright-reflecting
44 source regions, *IEEE Trans. Geosci.*, 42, 557-569, 2004.

1 Huang, J., Minnis, P., Lin, B., Wang, T., Yi, Y., Hu, Y., Sun-Mack, S., and Ayers, K.: Possible
2 influences of Asian dust aerosols on cloud properties and radiative forcing observed from MODIS
3 and CERES, *Geophys. Res. Lett.*, 33, L06824, 10.1029/2005GL024724, 2006.

4 Huang, J., Wang, T., Wang, W., Li, Z., and Yan, H.: Climate effects of dust aerosols over East
5 Asian arid and semiarid regions, *J. Geophys. Res.: Atmos.*, 119, 2014JD021796,
6 10.1002/2014JD021796, 2014.

7 Jiang, H., Farrar, J. T., Beardsley, R. C., Chen, R., and Chen, C.: Zonal surface wind jets across
8 the Red Sea due to mountain gap forcing along both sides of the Red Sea, *Geophys. Res. Lett.*, 36,
9 L19605, 10.1029/2009GL040008, 2009.

10 Jickells, T. D., An, Z. S., Andersen, K. K., Baker, A. R., Bergametti, G., Brooks, N., Cao, J. J.,
11 Boyd, P. W., Duce, R. A., Hunter, K. A., Kawahata, H., Kubilay, N., laRoche, J., Liss, P. S.,
12 Mahowald, N., Prospero, J. M., Ridgwell, A. J., Tegen, I., and Torres, R.: Global iron connections
13 between desert dust, ocean biogeochemistry, and climate, *Science*, 308, 67-71, 2005.

14 Kalenderski, S., Stenichkov, G., and Zhao, C.: Modeling a typical winter-time dust event over the
15 Arabian Peninsula and the Red Sea, *Atmos. Chem. Phys.*, 13, 1999-2014, 10.5194/acp-13-1999-
16 2013.

17 [Kandler, K., Schütz, L., Deutscher, C., Ebert, M., Hofmann, H., Jäckel, S., Jaenicke, R., Knippertz,](#)
18 [P., Lieke, K., Massling, A., Petzold, A., Schladitz, A., Weinzierl, B., Wiedensohler, A., Zorn, S.,](#)
19 [and Weinbruch, S.: Size distribution, mass concentration, chemical and mineralogical composition](#)
20 [and derived optical parameters of the boundary layer aerosol at Tinfou, Morocco, during SAMUM](#)
21 [2006, *Tellus*, 61B, 32-50, 2009.](#)

22
23
24
25

26 Kerr, P. F.: *Optical Mineralogy*, 3rd ed., McGraw-Hill Book Company, Inc., 442 pp., 1959.

27 Kok, J. F.: A scaling theory for the size distribution of emitted dust aerosols suggests climate
28 models underestimate the size of the global dust cycle, *Proc. Natl. Acad. Sci.*, 108, 1016–1021,
29 2011a.

30 Kok, J. F.: Does the size distribution of mineral dust aerosols depend on the wind speed at
31 emission?, *Atmos. Chem. Phys.*, 11, 10149–10156, 2011b.

32 Kumar, R., Barth, M. C., Pfister, G. G., Naja, M., and Brasseur, G. P.: WRF-Chem simulations of
33 a typical pre-monsoon dust storm in northern India: influences on aerosol optical properties and
34 radiation budget, *Atmos. Chem. Phys.*, 14, 2431-2446, 10.5194/acp-14-2431-2014, 2014.

35 ~~[Lee, S. Y., Dixon, J. B., and Abu Husayn, M. M.: Mineralogy of Saudi Arabian Soils: Eastern](#)~~
36 ~~[Region, *Soil Sci. Soc. Am. J.*, 47, 321–326, 10.2136/sssaj1983.03615995004700020030x, 1983.](#)~~

37 ~~[Leinen, M., Prospero, J. M., Arnold, E., and Blank, M.: Mineralogy of aeolian dust reaching the](#)~~
38 ~~[North Pacific Ocean 1. Sampling and analysis, *Journal of Geophysical Research*, 99, 21,017-](#)~~
39 ~~[021,023, 1994.](#)~~

40 Mahowald, N., S. Engelstaedter, C. Luo, A. Sealy, P. Artaxo, C. Benitez-Nelson, S. Bonnet, Y.
41 Chen, P.Y. Chuang, D.D. Cohen, F. Dulac, B. Herut, A.M. Johansen, N. Kubilay, R. Losno, W.
42 Maenhaut, A. Paytan, J.M. Prospero, L.M. Shank, and R.L. Siefert: Atmospheric iron deposition:
43 Global distribution, variability and human perturbations, *Ann. Rev. Marine Sci.*, 1, 245-278, 2009.

44 Marticorena, B., and Bergametti, G.: Modeling the atmospheric dust cycle: 1. Design of a soil-
45 derived dust emission scheme, *J. Geophys. Res.: Atmos.*, 100, 16415-16430, 10.1029/95JD00690,
46 1995.

1 Marticorena, B.: Dust production mechanisms, in: Mineral Dust: A Key Player in the Earth
2 System, edited by: Knippertz, P., and Stuut, J.-B. W., Springer Science+Business Media
3 Dordrecht, 93-120, 2014.

4 Menéndez, I., Pérez-Chacón, E., Mangas, J., Tauler, E., Engelbrecht, J. P., Derbyshire, E., Cana,
5 L., and Alonso, I.: Dust deposits on La Graciosa Island (Canary Islands, Spain): Texture,
6 mineralogy and a case study of recent dust plume transport, *Catena*, 117, 133-144, 2014.

7 Menut, L., Pérez, C., Haustein, K., Bessagnet, B., Prigent, C., and Alfaro, S.: Impact of surface
8 roughness and soil texture on mineral dust emission fluxes modeling, *J. Geophys. Res.: Atmos.*,
9 118, 6505-6520, 10.1002/jgrd.50313, 2013.

10 Migon, C., Sandroni, V., and Béthoux, J. P.: Atmospheric input of anthropogenic phosphorus to
11 the northwest Mediterranean under oligotrophic conditions, *Mar. Environ. Res.*, 7, 1-14., 2001.

12 Moosmüller, H., Engelbrecht, J. P., Skiba, M., Frey, G., Chakrabarty, R. K., and Arnott, W. P.:
13 Single scattering albedo of fine mineral dust aerosols controlled by iron concentration, *J. Geophys.*
14 *Res.*, 117, D11210, doi:10.1029/2011JD016909, 10.1029/2011JD016909, 2012.

15 Muhs, D. R., Prospero, J. M., Baddock, M. C., and Gill, T. E.: Identifying sources of aeolian
16 mineral dust: Present and past, in: Mineral Dust, A Key Player in the Earth System, edited by:
17 Knippertz, P., and Stuut, J.-B. W., Springer Science+Business Media Dordrecht, 51-74, 2014.

18 Nickovic, S., Vukovic, A., Vujadinovic, M., Djurdjevic, V., and Pejanovic, G.: Technical Note:
19 High-resolution mineralogical database of dust-productive soils for atmospheric dust modeling,
20 *Atmos. Chem. Phys.*, 12, 845–855, 2012.

21 Nihlen, T., and Lund, S. O.: Influence of Aeolian Dust on Soil Formation in the Aegean Area, *Z.*
22 *Geomorphol.*, 393, 341-361, 1995.

23 Oleson, K. W., Lawrence, D. M., Bonan, G. B., Flanner, M. G., Kluzek, E., Lawrence, P. J., Levis,
24 S., Swenson, S. C., Thornton, P. E., Dai, A., Decker, M., Dickinson, R., Feddema, J., Heald, C. L.,
25 Hoffman, F., Lamarque, J., Mahowald, N., Niu, G., Qian, T., Randerson, J., Running, S.,
26 Sakaguchi, K., Slater, A., Stockli, R., Wang, A., Yang, Z., Zeng, X., and Zeng, X.: Technical
27 Description of version 4.0 of the Community Land Model (CLM). , NCAR Technical Note
28 NCAR/TN-478+STR, 2010.

29 Osipov, S., Stenchikov, G., Brindley, H., and Banks, J.: Diurnal cycle of the dust instantaneous
30 direct radiative forcing over the Arabian Peninsula, *Atmos. Chem. Phys.*, 15, 9537-9553,
31 10.5194/acp-15-9537-2015, 2015.

32 Perlwitz, J. P., Pérez García-Pando, C., and Miller, R. L.: Predicting the mineral composition of
33 dust aerosols – Part 2: Model evaluation and identification of key processes with observations,
34 *Atmos. Chem. Phys.*, 15, 11629-11652, 10.5194/acp-15-11629-2015, 2015a.

35 Perlwitz, J. P., Pérez García-Pando, C., and Miller, R. L.: Predicting the mineral composition of
36 dust aerosols – Part 1: Representing key processes, *Atmos. Chem. Phys.*, 15, 11593-11627,
37 10.5194/acp-15-11593-2015, 2015b.

38 Prakash, J. P., Stenchikov, G., Kalenderski, S., Osipov, S., and Bangalath, H.: The impact of dust
39 storms on the Arabian Peninsula and the Red Sea, *Atmos. Chem. Phys.*, 15, 199-222, 10.5194/acp-
40 15-199-2015, 2015.

41 Prospero, J. M., Ginoux, P., Torres, O., Nicholson, S. E., and Gill, T. E.: Environmental
42 characterization of global sources of atmospheric soil dust identified with the NIMBUS 7 total
43 ozone mapping spectrometer (TOMS) absorbing aerosol product, *Rev. Geophys.*, 40, 31,
44 10.1029/2000RG000095, 2002.

45 [Pye, K.: Aeolian dust and dust deposits, Academic Press, London, 1987.](#)[Roquin, C., Freyssinet,](#)
46 [P., Zeegers, H., and Tardy, Y.: Element distribution patterns in laterites of southern Mali:](#)

1 [Consequence for geochemical prospecting and mineral exploration, *Applied Geochemistry*, 5,](#)
2 [303-315, 1990.](#)
3
4 Rietveld, H. M.: A profile refinement method for nuclear and magnetic structures, *J. Appl.*
5 *Crystallogr.*, 2, 65-71, [dx.doi.org/10.1107/S0021889869006558](https://doi.org/10.1107/S0021889869006558), 1969.
6 Scheuven, D., and Kandler, K.: On composition, morphology, and size distribution of airborne
7 mineral dust, in: *Mineral Dust, a Key Player in the Earth System*, edited by: Knippertz, P., and
8 Stuu, J.-B. W., Springer Science+Business Media Dordrecht, 15-49, 2014.
9 Shadfan, H., Mashhady, A., Eter, A., and Hussen, A. A.: Mineral composition of selected soils in
10 Saudi Arabia, *J. Plant Nutr. Soil Sci.*, 147, 657-668, [10.1002/jpln.19841470603](https://doi.org/10.1002/jpln.19841470603), 1984.
11 Sokolik, I. N., and Toon, O. B.: Direct radiative forcing by anthropogenic airborne mineral
12 aerosols, *Nature*, 381, 681-683, 1996.
13 Sokolik, I. N., and Toon, O. B.: Incorporation of mineralogical composition into models of the
14 radiative properties of mineral aerosol from UV to IR wavelengths, *J. Geophys. Res.: Atmos.*, 104,
15 9423-9444, [10.1029/1998JD200048](https://doi.org/10.1029/1998JD200048), 1999.
16 Sturges, W. T., Harrison, R. M., and Barrie, L. A.: Semi-quantitative X-ray diffraction analysis of
17 size fractionated atmospheric particles, *Atmos. Env.*, 23, 1083-1098, 1989.
18 Tanaka, T. Y., and Chiba, M.: A numerical study of the contributions of dust source regions to the
19 global dust budget, *Global Planet. Change*, 52, 88-104, 2006.
20 Tegen, I., and Fung, I.: Contribution to the atmospheric mineral aerosol load from land surface
21 modification, *J. Geophys. Res.*, 100, 18707-18726, 1995.
22 Twomey, S. A., Piepgrass, M., and Wolfe, T. L.: An assessment of the impact of pollution on
23 global cloud albedo, *Tellus B*, 36, [10.3402/tellusb.v36i5.14916](https://doi.org/10.3402/tellusb.v36i5.14916), 2011.
24 UCAR/NCAR: Forecasting Dust Storms, National Center for Atmospheric Research, Boulder,
25 National Center for Atmospheric Research, Boulder, 1-67, 2003.
26 Viani, B. E., A. S. Al-Mashhady, and Dixon, J. B.: Mineralogy of Saudi Arabian Soils: Central
27 Alluvial Basins, *Soil Sci. Soc. Am. J.*, 47, 149-157, [10.2136/sssaj1983.03615995004700010030x](https://doi.org/10.2136/sssaj1983.03615995004700010030x),
28 1983.
29 Wang, W., Huang, J., Minnis, P., Hu, Y., Li, J., Huang, Z., Ayers, J. K., and Wang, T.: Dusty
30 cloud properties and radiative forcing over dust source and downwind regions derived from A-
31 Train data during the Pacific Dust Experiment, *J. Geophys. Res.: Atmos.*, 115, D00H35,
32 [10.1029/2010JD014109](https://doi.org/10.1029/2010JD014109), 2010.
33 Wang, Z., Ueda, H., and Huang, M.: A deflation module for use in modeling long-range transport
34 of yellow sand over East Asia, *J. Geophys. Res.: Atmos.*, 105, 26947-26959,
35 [10.1029/2000JD900370](https://doi.org/10.1029/2000JD900370), 2000.
36 Washington, R., Todd, M. C., Middleton, N. J., and Goudie, A. S.: Dust-storm source areas
37 determined by the total ozone monitoring spectrometer and surface observations, *Ann. Assoc. Am.*
38 *Geogr.*, 93, 297-313, 2003.
39 Washington, R., and Todd, M. C.: Atmospheric controls on mineral dust emission from the Bodélé
40 depression, Chad: The role of the low level jet, *Geophys. Res. Lett.*, 32, L17701,
41 [doi:10.1029/2005GL023597](https://doi.org/10.1029/2005GL023597), 2005.
42 Webb, N. P., and Strong, C. L.: Soil erodibility dynamics and its representation for wind erosion
43 and dust emission models, *Aeolian Res.*, 3, 165-179, [10.1016/j.aeolia.2011.03.002](https://doi.org/10.1016/j.aeolia.2011.03.002), 2011.
44 Weese, C. B., and Abraham, J. H.: Potential health implications associated with particulate matter
45 exposure in deployed settings in Southwest Asia, *Inhalation Toxicol.*, 21, 291-296, 2009.

- 1 Zender, C. S., Huisheng, B., and David, N.: Mineral Dust Entrainment and Deposition (DEAD)
- 2 model: Description and 1990s dust climatology, *J. Geophys. Res.: Atmos.*, 108, 2003.

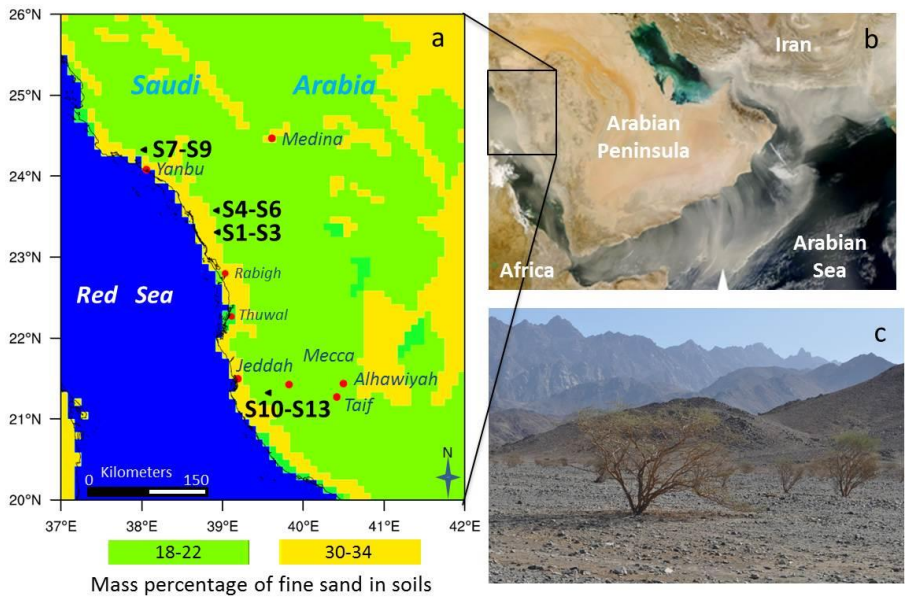
Table 1. Localities of soil sampling sites along the Red Sea coastal plain.

Site	Proximity	Latitude	Longitude	Elevation (m)
S1	SE of Al Nasaif	23.3322° N	38.9481° E	94
S2	SE of Al Nasaif	23.2961° N	38.9385° E	68
S3	SE of Al Nasaif	23.2920° N	38.9100° E	46
S4	E of Ar Rayis	23.5876° N	38.9243° E	128
S5	E of Ar Rayis	23.5746° N	38.9213° E	118
S6	E of Ar Rayis	23.5656° N	38.9193° E	115
S7	N of Yanbu	24.3334° N	38.0205° E	113
S8	N of Yanbu	24.3239° N	38.0254° E	60
S9	N of Yanbu	24.3195° N	38.0245° E	56
S10	SW of Mecca	21.3197° N	39.5763° E	128
S11	SW of Mecca	21.3232° N	39.5711° E	124
S12	SW of Mecca	21.3211° N	39.5593° E	133
S13	SW of Mecca	21.3253° N	39.5508° E	118

Table 2. The volume particle size fraction (%) of the D < 600 µm sieved soil samples.

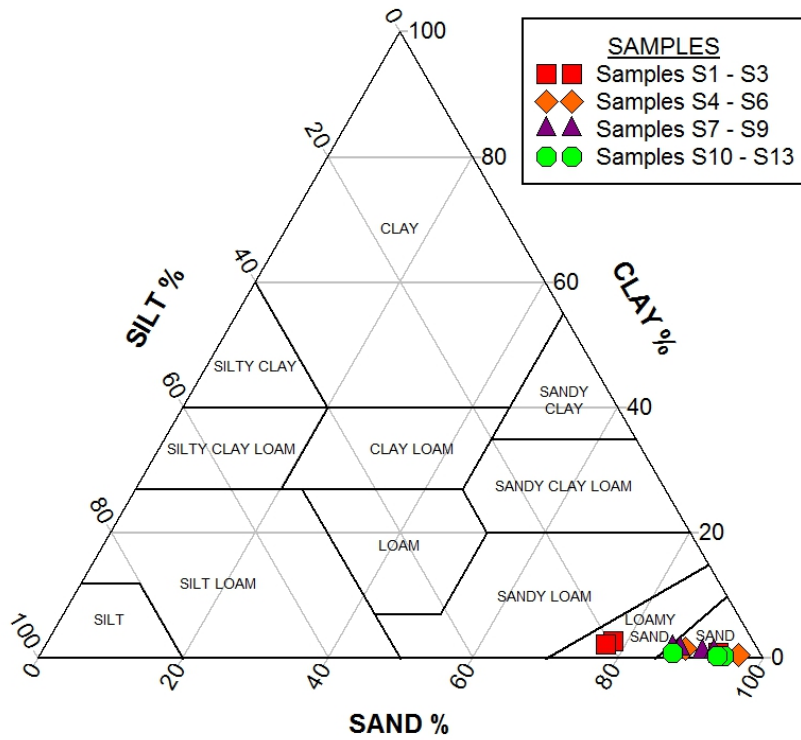
Sample	Sand (600–62.5 µm)	Silt (62.5–2 µm)	Clay (< 2 µm)
S1	78.0	19.2	2.8
S2	77.2	20.5	2.3
S3	93.3	5.7	1.0
S4	96.3	3.0	0.7
S5	88.4	10.0	1.7
S6	88.5	9.8	1.6
S7	94.3	5.2	0.5
S8	93.5	6.0	0.5
S9	87.1	12.1	0.9
S10	87.8	10.6	1.6
S11	86.6	11.4	1.9
S12	91.1	7.6	1.2
S13	92.7	6.1	1.2

1
2
3



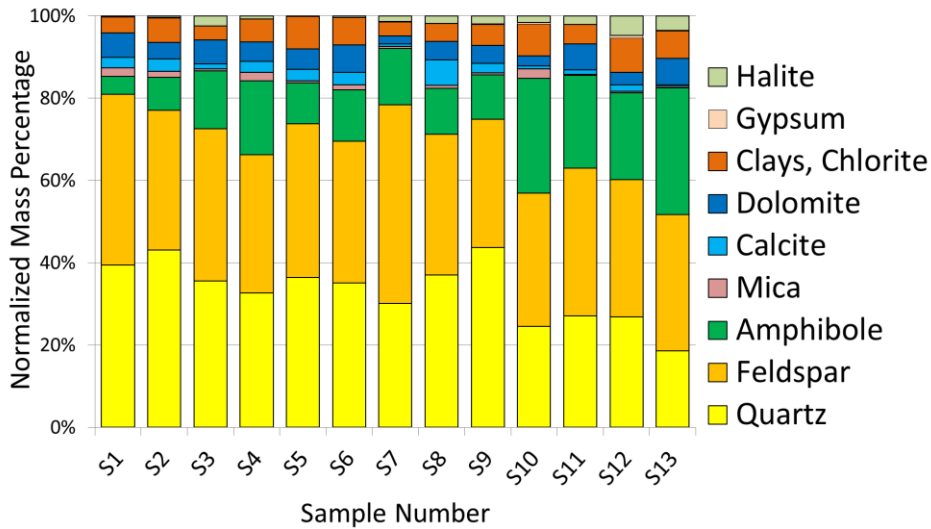
4
5
6
7
8
9
10
11
12
13
14
15
16

Fig. 1 (a) Map showing the mass percentage of fine sand in soils, based on STATSGO-FAO soil texture data (Nickovic et al., 2012; Menut et al., 2013), in the Arabian Peninsula, as well as the four localities and thirteen (S1–S13) sampling sites. **(b)** Modis satellite image of dust storm over the Arabian Peninsula captured on February 22, 2008 (NASA Modis web site). **(c)** Sampling site S1 showing the typical acacia trees growing along the wadi in the foreground, with the Hejaz mountain range and escarpment in the distance.



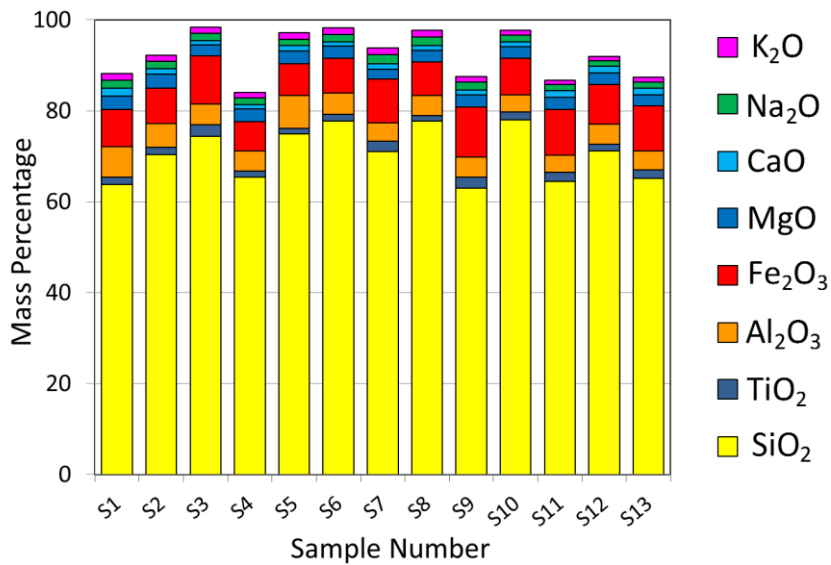
1
 2 **Fig 2.** US Department of Agriculture (USDA) soil textural triangle showing the grain size plot of
 3 the thirteen samples collected for this study. Volume size-class fractions grouped as clay (< 2
 4 μm), silt (2 – 62.5 μm) and sand (62.5 – 600 μm).

5
 6
 7
 8
 9
 10

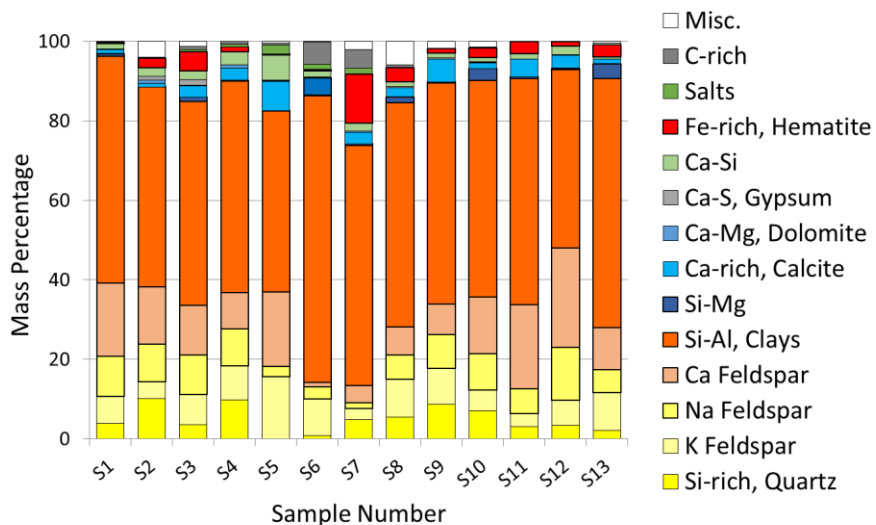


1
 2 **Fig 3.** Normalized mineral compositions by percentage of mass [quartz (19 – 44%), feldspars
 3 (plagioclase, K-feldspar) (31 – 48%), amphibole and pyroxene (4 – 31%), calcite (0.4 – 6.2%),
 4 dolomite (1.9 – 6.6%), clays and chlorite (smectite, illite, palygorskite, kaolinite) (3.3 – 8.3%),
 5 gypsum (0 – 0.6%) and halite (0.2 – 4.8%)] of thirteen D < 38µm sieved soil samples collected at
 6 four localities along the Red Sea coastal area, as measured by X-ray diffraction
 7 (XRD). Normalized mineral compositions of thirteen D < 38µm sieved soil samples collected at
 8 four localities along the Red Sea coastal area, as measured by X-ray diffraction (XRD).
 9

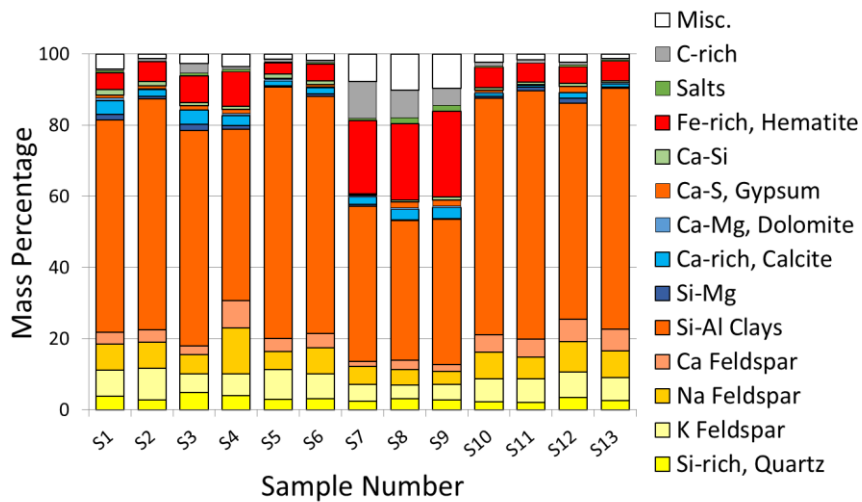
10
 11
 12
 13
 14
 15
 16
 17



1
 2 **Fig. 4.** Compositional plot showing major oxides percentages by mass [SiO₂ (63 – 78%), TiO₂
 3 (1.2 – 2.5 %), Al₂O₃ (3.7 – 7.3 %), Fe₂O₃ (6.5 – 11 %), MgO (2.3 – 3.1 %), CaO (0.9 – 1.7 %),
 4 Na₂O (1.2 – 2.0 %), K₂O (0.9 – 1.6 %)] from ICP-OES analysis of < 38 μm sieved
 5 soils
 6
 7
 8
 9
 10
 11
 12
 13

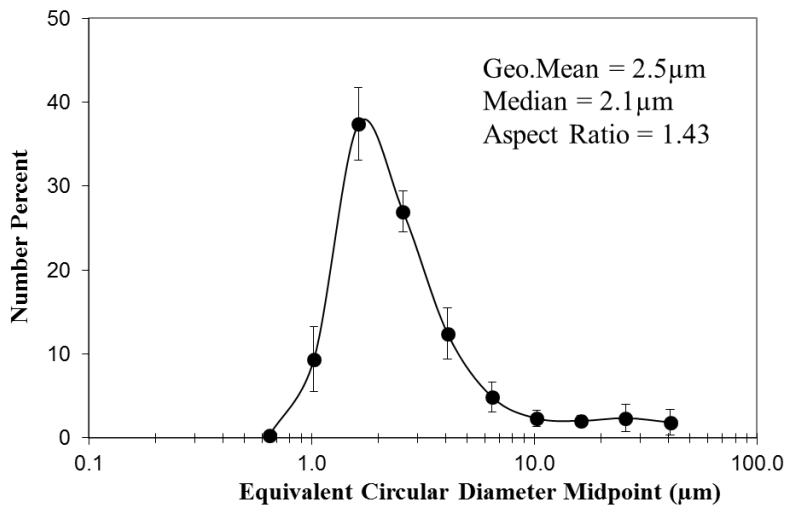


1
2 **Fig. 5. CCSEM based individual particle analysis for 0.5 – 38 μm chemical set, with the**
3 **chemical bins labeled as minerals by normalized mass percentage [Si-rich, Quartz (0.1 – 10.2**
4 **%), K Feldspar (2.7 – 15.6 %), Ca Feldspar (1.1 – 25 %); Na Feldspar (1.5 – 13.4 %); Si-Al,**
5 **Clays (44.7 – 72.1 %); Si-Mg (0 – 3.7 %); Ca-Mg, Dolomite (0 – 0.8 %); Ca-Si (0.6 – 6.4 %);**
6 **Ca-S, Gypsum (0 – 1.5 %); Ca-rich, Calcite (0.9 – 7.4 %); Fe-rich, Hematite (0.2 – 12.4 %);**
7 **Salts (0 – 2.2 %); C-rich (0 – 5.5 %) and Misc.(0 – 5.9 %)]CCSEM based individual particle**
8 **analysis for 0.5 – 38 μm chemical set, with the chemical bins labeled as minerals.**
9
10
11
12
13
14
15
16
17
18



1
2 **Fig. 6.** CCSEM based individual particle analysis for 0.5 – 2.5 μm (fine) subset, with the
3 chemical bins labeled as minerals by normalized mass percentage [Si-rich, Quartz (2.1 – 4.9 %),
4 K Feldspar (3.8 – 9.0 %), Na Feldspar (3.8 – 12.9 %); Ca Feldspar (1.4 – 7.7 %); Si-Al, Clays
5 (39.2 – 70.7 %); Si-Mg (0.2 – 1.7 %); Ca-Mg, Dolomite (0 – 0.7 %); Ca-Si (0.3 – 1.5 %); Ca-S,
6 Gypsum (0.1 – 1.7 %); Ca-rich, Calcite (0.6 – 4.1 %); Fe-rich, Hematite (3.2 – 24.1 %); Salts
7 (0.1 – 1.6 %); C-rich (0.4 – 10.5 %) and Miscellaneous.(1.2 – 10.1 %)]
8 CCSEM based individual particle analysis for 0.5 – 2.5 μm (fine) subset, with the chemical bins
9 labeled as minerals.

10
11
12
13
14
15
16
17
18



1
2 **Fig. 7.** Average and standard deviations of particle sizes, as well as size and shape statistics for
3 thirteen $D < 38 \mu\text{m}$ sieved samples, as measured by scanning electron microscopy (CCSEM).
4

5
6
7
8
9
10
11
12
13
14 **Appendix A€**

15 **Table A€1.** Major, minor and trace element compositions by Inductively Coupled Plasma
16 Optical Emission Spectrometry (ICP-OES), and water soluble ions by Ion Chromatography (IC)
17 of grab samples, S1 to S3 collected near Al Nasaif, and S4 to S6 collected near Ar Rayis, all
18 along the Red Sea coastal region. Also tabulated are elemental mass ratios, statistics of the
19 individual particle sizes and morphology as measured by CCSEM.
20

Sample #	S1		S2		S3		S4		S5		S6	
Major and minor elements as oxides (%)												
	Conc.	Unc.	Conc.	Unc.	Conc.	Unc.	Conc.	Unc.	Conc.	Unc.	Conc.	Unc.
SiO ₂	63.795 ± 3.190		70.302 ± 3.515		74.337 ± 3.717		65.436 ± 3.272		74.872 ± 3.744		77.668 ± 3.883	
TiO ₂	1.577 ± 0.079		1.700 ± 0.085		2.536 ± 0.127		1.300 ± 0.065		1.237 ± 0.062		1.511 ± 0.076	
Al ₂ O ₃	6.768 ± 0.338		5.195 ± 0.260		4.664 ± 0.233		4.367 ± 0.218		7.260 ± 0.363		4.710 ± 0.236	
Fe ₂ O ₃	8.195 ± 0.410		7.777 ± 0.389		10.497 ± 0.525		6.535 ± 0.327		6.936 ± 0.347		7.584 ± 0.379	
MnO	0.112 ± 0.006		0.119 ± 0.006		0.135 ± 0.007		0.109 ± 0.005		0.123 ± 0.006		0.144 ± 0.007	
MgO	2.903 ± 0.145		3.137 ± 0.157		2.478 ± 0.124		2.741 ± 0.137		2.824 ± 0.141		2.767 ± 0.138	
CaO	1.723 ± 0.086		1.200 ± 0.060		0.895 ± 0.045		0.900 ± 0.045		1.249 ± 0.062		0.909 ± 0.045	
Na ₂ O	1.695 ± 0.085		1.577 ± 0.079		1.657 ± 0.083		1.494 ± 0.075		1.248 ± 0.062		1.659 ± 0.083	
K ₂ O	1.473 ± 0.074		1.372 ± 0.069		1.269 ± 0.063		1.198 ± 0.060		1.579 ± 0.079		1.484 ± 0.074	
P ₂ O ₅	0.406 ± 0.048		0.353 ± 0.047		0.400 ± 0.048		0.364 ± 0.048		0.291 ± 0.046		0.403 ± 0.048	
Total	88.649		92.734		98.867		84.444		97.620		98.838	
Trace elements (ppm)												
Li	17 ± 1		21 ± 1		15 ± 1		19 ± 1		24 ± 1		22 ± 1	
V	183 ± 9		182 ± 9		242 ± 12		161 ± 8		166 ± 8		191 ± 10	
Cr	114 ± 6		103 ± 5		150 ± 8		83 ± 4		91 ± 5		98 ± 5	
Co	30 ± 1		27 ± 1		26 ± 1		29 ± 1		28 ± 1		29 ± 1	
Ni	55 ± 3		52 ± 3		46 ± 2		45 ± 2		48 ± 2		50 ± 3	
Cu	29 ± 1		33 ± 2		24 ± 1		42 ± 2		40 ± 2		42 ± 2	
Zn	39 ± 2		39 ± 2		40 ± 2		39 ± 2		47 ± 2		90 ± 5	
Sr	294 ± 16		333 ± 18		358 ± 19		288 ± 15		285 ± 15		306 ± 16	
Ba	318 ± 16		426 ± 21		342 ± 17		408 ± 20		502 ± 25		610 ± 30	
Water soluble ions (%)												
Mg ²⁺	0.046 ± 0.001		0.038 ± 0.001		0.027 ± 0.001		0.036 ± 0.001		0.044 ± 0.001		0.143 ± 0.004	
Ca ²⁺	0.171 ± 0.022		0.106 ± 0.014		0.071 ± 0.009		0.107 ± 0.014		0.162 ± 0.021		0.455 ± 0.058	
Na ⁺	0.024 ± 0.001		0.005 ± 0.001		0.007 ± 0.001		0.005 ± 0.001		0.008 ± 0.001		0.025 ± 0.003	
K ⁺	0.020 ± 0.002		0.010 ± 0.001		0.008 ± 0.001		0.011 ± 0.001		0.025 ± 0.002		0.037 ± 0.004	
Cl ⁻	0.092 ± 0.004		0.000 ± 0.001		0.000 ± 0.001		0.000 ± 0.001		0.040 ± 0.002		0.222 ± 0.010	
SO ₄ ²⁻	0.078 ± 0.001		0.031 ± 0.001		0.017 ± 0.001		0.126 ± 0.002		0.131 ± 0.002		0.466 ± 0.007	
PO ₄ ³⁻	0.002 ± 0.001		0.002 ± 0.001		0.000 ± 0.001		0.000 ± 0.001		0.002 ± 0.001		0.006 ± 0.004	
NO ₃ ⁻	0.018 ± 0.002		0.006 ± 0.001		0.011 ± 0.001		0.016 ± 0.002		0.019 ± 0.002		0.076 ± 0.007	
Mass ratios												
Si/Al	8.321		11.946		14.071		13.227		9.105		14.558	
Ca/Al	0.344		0.312		0.259		0.279		0.233		0.261	
Fe/Al	1.600		1.978		2.974		1.977		1.262		2.128	
Particle diameter from CCSEM measurements (approx. 2000 particles)(µm)												
Geom. Mean (µm)	2.81		2.12		3.50		2.24		2.53		2.35	
Arith. Mean (µm)	3.66		2.72		6.75		3.25		3.29		3.00	
Skewness	4.57		4.32		2.34		5.04		5.44		5.51	
Kurtosis	28.85		25.20		4.63		29.43		40.11		44.00	
Mean aspect ratio	1.41		1.42		1.48		1.45		1.41		1.41	

1
2
3

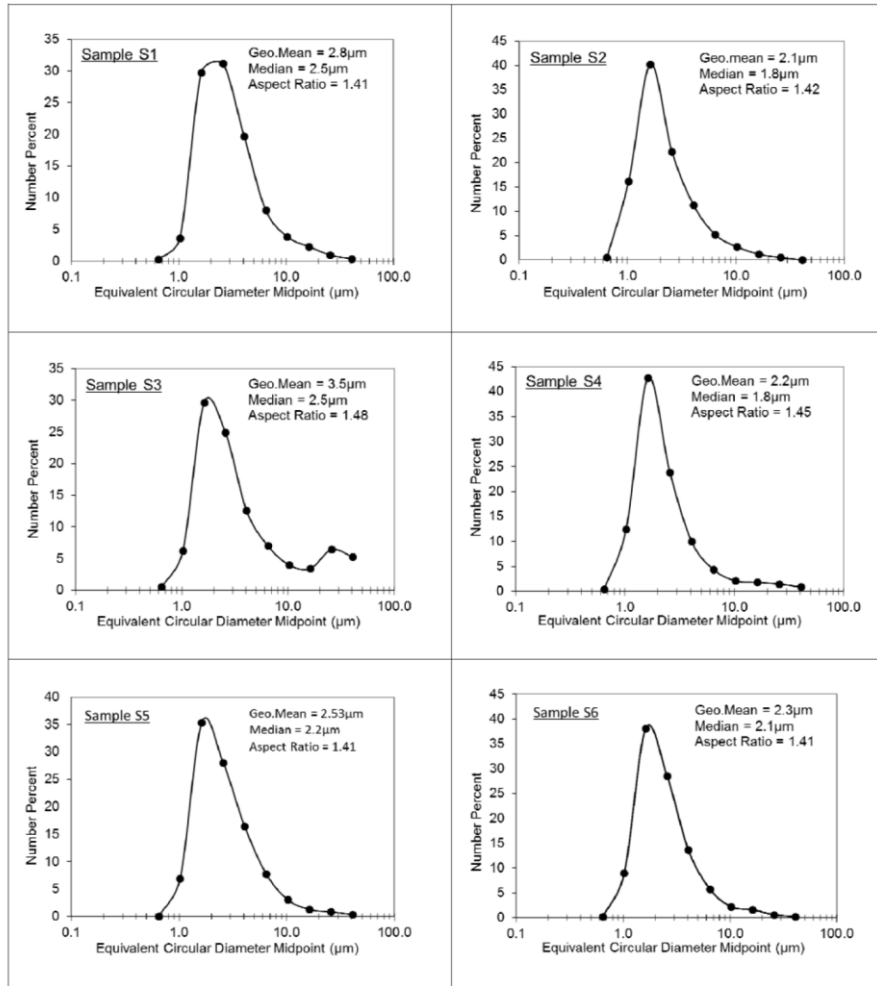
Appendix A6

Table A6.2. Major, minor and trace element compositions by Inductively Coupled Plasma Optical Emission Spectrometry (ICP-OES), and water soluble ions by Ion Chromatography (IC) of grab samples S7 to S9 collected near Yanbu, and S10 to S13 near Mecca, all along the Red Sea coastal region. Also tabulated are elemental mass ratios, statistics of the individual particle size and morphology as measured by CCSEM.

Sample #	S7		S8		S9		S10		S11		S12		S13	
Major and minor elements as oxides (%)														
	Conc.	Unc.	Conc.	Unc.	Conc.	Unc.	Conc.	Unc.	Conc.	Unc.	Conc.	Unc.	Conc.	Unc.
SiO ₂	71.041 ± 3.552		77.76 ± 3.888		62.997 ± 3.150		78.006 ± 3.900		64.44 ± 3.222		71.091 ± 3.555		65.173 ± 3.259	
TiO ₂	2.246 ± 0.112		1.22 ± 0.061		2.401 ± 0.120		1.793 ± 0.090		2.09 ± 0.104		1.499 ± 0.075		1.786 ± 0.089	
Al ₂ O ₃	4.080 ± 0.204		4.33 ± 0.217		4.351 ± 0.218		3.697 ± 0.185		3.70 ± 0.185		4.516 ± 0.226		4.198 ± 0.210	
Fe ₂ O ₃	9.563 ± 0.478		7.43 ± 0.371		11.027 ± 0.551		7.997 ± 0.400		10.07 ± 0.504		8.604 ± 0.430		9.936 ± 0.497	
MnO	0.121 ± 0.006		0.10 ± 0.005		0.156 ± 0.008		0.126 ± 0.006		0.13 ± 0.007		0.115 ± 0.006		0.117 ± 0.006	
MgO	2.255 ± 0.113		2.53 ± 0.127		2.76 ± 0.138		2.549 ± 0.127		2.62 ± 0.131		2.556 ± 0.128		2.345 ± 0.117	
CaO	1.109 ± 0.055		1.02 ± 0.051		1.071 ± 0.054		1.064 ± 0.053		1.55 ± 0.077		1.547 ± 0.077		1.586 ± 0.079	
Na ₂ O	2.015 ± 0.101		1.92 ± 0.096		1.638 ± 0.082		1.485 ± 0.074		1.31 ± 0.066		1.248 ± 0.062		1.255 ± 0.063	
K ₂ O	1.495 ± 0.075		1.49 ± 0.074		1.335 ± 0.067		1.059 ± 0.053		0.96 ± 0.048		0.942 ± 0.047		1.040 ± 0.052	
P ₂ O ₅	0.467 ± 0.050		0.452 ± 0.049		0.461 ± 0.050		0.385 ± 0.048		0.446 ± 0.049		0.384 ± 0.048		0.384 ± 0.048	
Total	94.392		98.250		88.192		98.160		87.326		92.503		87.819	
Trace elements (ppm)														
Li	16 ± 1		17 ± 1		19 ± 1		14 ± 1		14 ± 1		13 ± 1		12 ± 1	
V	215 ± 11		157 ± 8		257 ± 13		216 ± 11		283 ± 14		229 ± 11		284 ± 14	
Cr	129 ± 6		94 ± 5		167 ± 8		142 ± 7		177 ± 9		149 ± 7		171 ± 9	
Co	26 ± 1		25 ± 1		29 ± 1		31 ± 2		35 ± 2		36 ± 2		32 ± 2	
Ni	47 ± 2		46 ± 2		53 ± 3		58 ± 3		65 ± 3		61 ± 3		59 ± 3	
Cu	21 ± 1		22 ± 1		24 ± 1		52 ± 3		55 ± 3		58 ± 3		47 ± 2	
Zn	41 ± 2		38 ± 2		44 ± 2		41 ± 2		42 ± 2		42 ± 2		39 ± 2	
Sr	233 ± 13		180 ± 11		381 ± 20		281 ± 15		267 ± 14		259 ± 14		199 ± 11	
Ba	306 ± 15		302 ± 15		404 ± 20		430 ± 21		409 ± 20		407 ± 20		323 ± 16	
Water soluble ions (%)														
Mg ²⁺	0.024 ± 0.001		0.024 ± 0.001		0.026 ± 0.001		0.025 ± 0.001		0.025 ± 0.001		0.025 ± 0.001		0.028 ± 0.001	
Ca ²⁺	0.139 ± 0.018		0.138 ± 0.018		0.126 ± 0.016		0.105 ± 0.018		0.061 ± 0.008		0.081 ± 0.010		0.073 ± 0.009	
Na ⁺	0.019 ± 0.001		0.012 ± 0.000		0.009 ± 0.001		0.008 ± 0.000		0.009 ± 0.001		0.009 ± 0.001		0.019 ± 0.001	
K ⁺	0.016 ± 0.001		0.014 ± 0.001		0.016 ± 0.001		0.016 ± 0.001		0.012 ± 0.001		0.016 ± 0.001		0.018 ± 0.001	
Cl ⁻	0.046 ± 0.002		0.037 ± 0.002		0.026 ± 0.001		0.000 ± 0.002		0.000 ± 0.001		0.000 ± 0.001		0.000 ± 0.001	
SO ₄ ²⁻	0.088 ± 0.001		0.056 ± 0.001		0.038 ± 0.001		0.091 ± 0.001		0.049 ± 0.001		0.070 ± 0.001		0.063 ± 0.001	
PO ₄ ³⁻	0.002 ± 0.001		0.001 ± 0.001		0.000 ± 0.001		0.001 ± 0.001		0.001 ± 0.001		0.001 ± 0.001		0.002 ± 0.001	
NO ₃ ⁻	0.014 ± 0.001		0.009 ± 0.001		0.005 ± 0.001		0.024 ± 0.001		0.012 ± 0.001		0.017 ± 0.002		0.016 ± 0.001	
Mass ratios														
Si/Al	15.370		15.846		12.782		18.628		15.368		13.896		13.705	
Ca/Al	0.367		0.318		0.333		0.389		0.564		0.463		0.511	
Fe/Al	3.097		2.266		3.349		2.858		3.595		2.517		3.127	
Particle diameter from CCSEM measurements (approx. 2000 particles)(µm)														
Geom. Mean (µm)	2.68		2.43		2.55		2.21		2.52		2.63		2.82	
Arith. Mean (µm)	4.50		4.18		4.47		3.67		4.05		4.17		4.94	
Skewness	3.61		3.83		3.63		4.35		4.21		3.93		3.34	
Kurtosis	13.38		14.87		13.14		19.06		18.56		16.74		11.20	
Mean aspect ratio														
	1.40		1.46		1.43		1.42		1.41		1.43		1.41	

8
9
10

Supplementary Information Appendix B



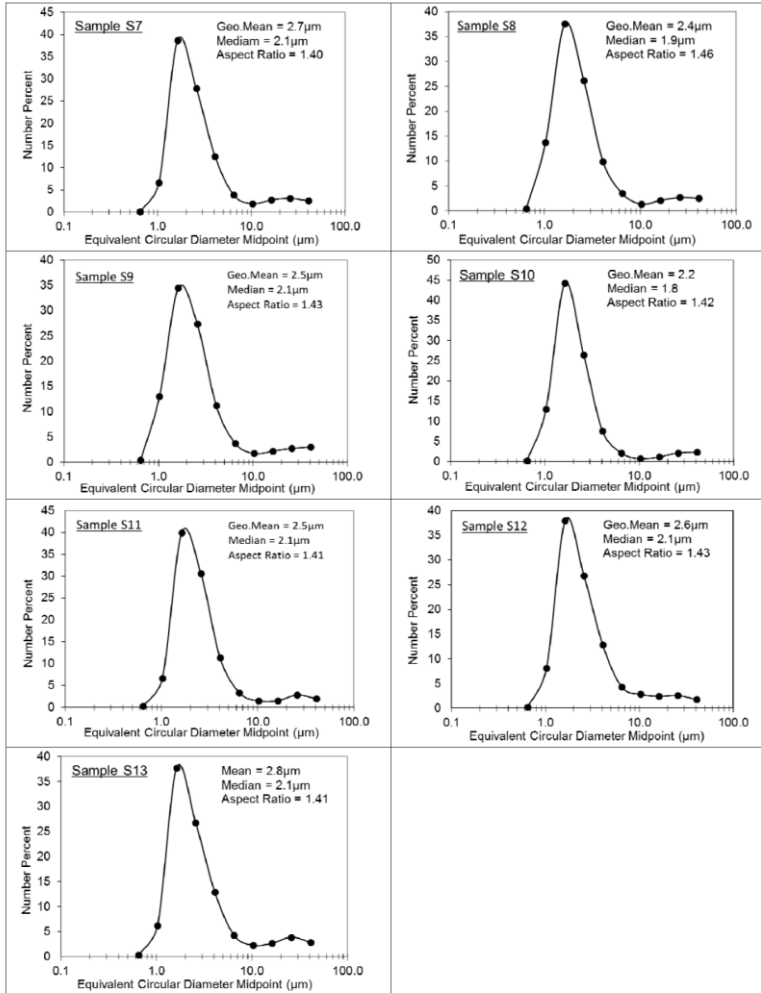
2

3 **S01Fig-B1.** Particle size distributions, as well as size and shape statistics for D<38 μm sieved
 4 samples S1 – S6, as measured by scanning electron microscopy (SEM).

5

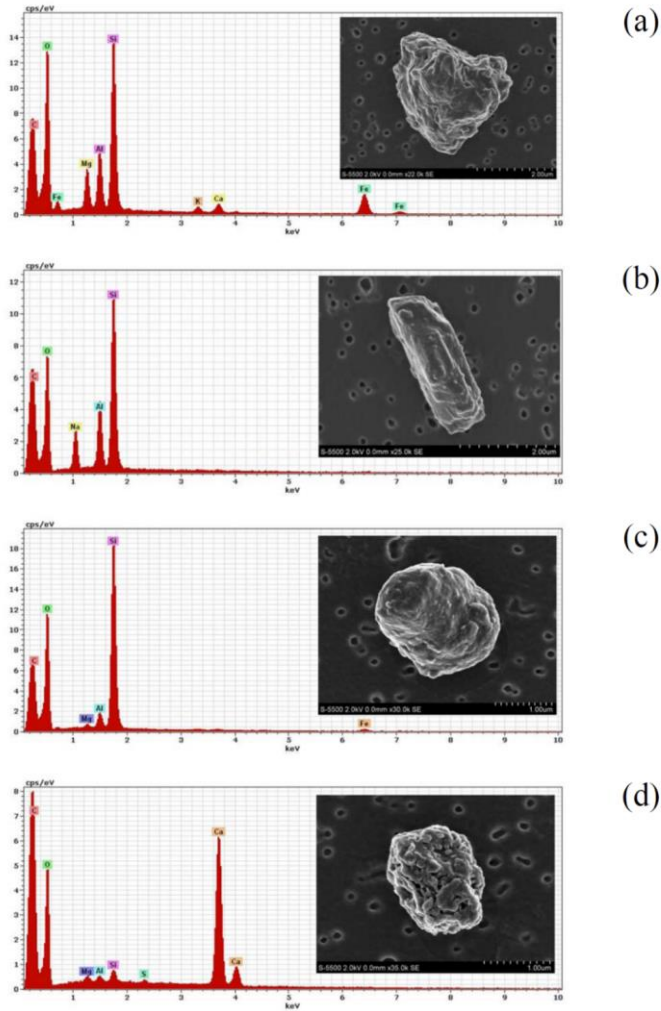
6

7



1
 2 **S02Fig. B2.** Particle size distributions, as well as size and shape statistics for D<38 μm sieved
 3 samples S7 – S13, as measured by scanning electron microscopy (SEM).
 4

Appendix B



2

3 **S03Fig-B3.** Secondary electron images and energy dispersive spectra (EDS) of soil particles (a)
 4 sample S5, Fe bearing clay mineral possibly illite. (b) sample S8, albite feldspar crystal. (c)
 5 sample S11, rounded quartz grain with minor amount of clay. (d) sample S11, cluster of calcite
 6 crystals with small amounts of clay and gypsum.
 7